A model-based method for visualisation, monitoring and diagnosis of fouling in heat exchangers

E. Diaz-Bejarano[1,2], *F. Coletti*[2,3] and *S. Macchietto*[1,2]*

[1]Department of Chemical Engineering, Imperial College London, London SW7 2AZ, UK

[2]Hexxcell Ltd., Innovation Hub, Imperial College - White City Campus, 80 Wood Lane, London W12 0BZ, UK.

[3]College of Engineering, Design and Physical Sciences, Brunel University London, Uxbridge, UB8 3PH, UK

* s.macchietto@imperial.ac.uk

KEYWORDS: *fouling, inorganics, heat exchanger, monitoring, diagnosis, visualisation*.

ABSTRACT

A critical review of current methods for monitoring the performance of heat exchangers in the presence of fouling highlights a number of pitfalls. An improved analysis method and visualisation of operation data (the TH-λ plot) are proposed which enable to accurately and rapidly estimate the location and extent of fouling, the properties of the deposit and their impact on exchanger performance. The method uses advanced dynamic thermo-hydraulic models to analyse the data. The visualisation presents this information in a way easily interpreted by field engineers. The superior features are demonstrated on various applications where traditional methods give poor visibility or outright wrong information about underlying events. These include organic fouling deposition and ageing, incomplete cleaning, multi-component deposits and changes in fouling behaviour. First, the basic concepts are illustrated with idealised examples (constant inlet conditions, using simulated data). The approach is then applied

to three real refining cases studies, with pressure drop either measured or generated via soft-sensors. The results show that the advanced dynamic models used enable to properly integrate and interpret highly variable data measurements, explain complex underlying thermal and hydraulic effects, adequately monitor performance, and rapidly detect changes in fouling behaviour. The approach provides a new practical tool for monitoring of heat exchanger performance and early fouling diagnosis.

INTRODUCTION

Fouling of heat exchangers in oil refineries is a long-standing problem that leads to substantial fuel consumption, emission of greenhouse gases, economic penalties, operation difficulties, the need of periodic maintenance, and safety hazards[1,2]. Fouling of shell-and-tube heat exchangers in pre-heat trains (PHTs) reduces energy recovery and increases pressure drop. Maintaining the performance (thermal and hydraulic) of heat exchangers is essential to ensure production, maximize energy efficiency and reduce CO_2 emissions. Adequate monitoring of the state of the exchangers is crucial to assist in operational decisions with respect to fouling mitigation options and cleaning strategies, but also to detect and diagnose unexpected events and help in planning corrective actions.

Monitoring stands for the observation and estimation of the state of a system and its evolution based on available measurements. It aims to provide the process engineers with practical answers on the performance of equipment, identification of inefficiencies, and planning of operation, shutdowns and cleanings[3]. Monitoring of heat exchangers undergoing fouling refers to two aspects: a) the exchanger performance; b) the presence, location and extent of fouling. Performance depends on the process variability but also on the fouling state. Guidelines and methods for heat exchanger monitoring are provided in EPRI (1991)[4] and ASME (1995)[5], as reviewed by Kuppan[6].

The monitoring methods used in refineries are subject to (and restricted by) the measurements available in these facilities. Examples of typical PHT instrumentation can be found in the literature[7–9]. Temperatures and flowrates are the operating conditions more often measured in PHTs. Temperatures are measured at key points (e.g. tank, desalter, flash drum, inlet and outlet temperatures to/from the furnace – usually called Coil Inlet Temperature, CIT, and Coil Outlet Temperature, COT, respectively). Due to the cost attached to sensors and their maintenance (and in refinery applications, safety

considerations), only key heat exchangers (typically those with greater duty or undergoing severe fouling) have temperature measurements for the two inlet and two outlet streams, as required for monitoring. Pressure measurements are also taken at key points in the network. Differential pressure for individual heat exchangers is typically unavailable, but some refineries do collect such measurements[9, 10]. Some cases have been reported where pressure drop data is available in controlled fouling experiments[11–14].

Most monitoring indicators used in refinery PHTs are based on thermal aspects (*Heat transfer methods*) and, less commonly, on hydraulic aspects (*Pressure drop methods*). Methods in these two categories are discussed below and summarized in Table 1. Other fouling monitoring methods include ultrasonic techniques[33, 34] and corrosion monitors[35]. Visual inspection during dismantling is a key complementary activity in order to assess the state of the heat exchangers before and after cleaning. Purely data-driven (e.g. AI) based methods are not covered here as they have yet to establish a track record.

Heat transfer methods may be based on temperature measurements, heat duty or heat transfer coefficients**.** The simpler method monitors thermal performance based on the *temperature difference* (ΔT), i.e. the increase or decrease in temperature as the stream passes through the exchanger. This indicator avoids complex calculations and relies merely on primary measurements. However, it does not directly give indications of the exchanger heat duty and does not account for ΔT changes resulting from variations in flowrates. Based on this indicator, Wilson *et al.*[17] proposed plotting hot stream temperatures against cold stream temperatures to simultaneously visualize inlet and outlet temperatures and ΔT for all the exchangers in a network, in a Temperature Field Plot. The approach aims at comparing initial (clean) and final (fouled) state of the network, identifying the heat exchangers more severely affected, and visualizing where an exchanger operates relative to its fouling threshold.

In a second category, the calculation of the heat duty involves the temperatures, flowrate (on a mass basis) and heat capacity of at least one stream. Thermal performance is commonly evaluated in terms of the heat exchanger effectiveness, i.e. the ratio of heat duty, Q, to its *theoretical* maximum ($\varepsilon = Q/Q_{max}$)[36].

Table 1. Key performance indicators in monitoring of heat exchangers undergoing fouling

Indicator	Name	Measurements	Remarks	Reference
Heat transfer Methods				
ΔT	Temperature difference	T_{in}, T_{out}	Based on primary measurements, minimum calculations. Does not account for variations in flowrate.	9, 15, 16, 7
$\varepsilon = \Delta T/(T_{in}-t_{in})$	Thermal effectiveness	T_{in}, T_{out}	Based on measurements, minimum calculations. Does not account for variations in flowrate unless corrected as in ref.[3]	3, 18
$FI = (\varepsilon_c - \varepsilon)/(\varepsilon_c - \varepsilon_f)$	Fouling index	T_{in}, T_{out}	Requires NTU model. No information on exchanger thermal performance.	3
Q	Heat duty	T_{in}, T_{out}, $\dot{m}$	Calculation of sensible heat.	16
$\varepsilon = Q/Q_{max}$	Exchanger effectiveness	T_{in}, T_{out}, $\dot{m}$	Calculation of sensible heat. Normalization w.r.t. theoretical maximum.	19
Q/Q_c	Thermal efficiency	T_{in}, T_{out}, $\dot{m}$	Requires heat exchanger model. Normalization w.r.t. practical maximum.	20
R_f	Fouling resistance	T_{in}, T_{out}, $\dot{m}$	Most common method. Requires heat exchanger model (usually LMTD). No information on exchanger thermal performance.	7, 8, 21–23
U	Overall HTC	T_{in}, T_{out}, $\dot{m}$	Requires heat exchanger model (usually LMTD). No information on exchanger thermal performance.	13, 24
CF = U/Uc	Cleanliness factor	T_{in}, T_{out}, $\dot{m}$	Requires heat exchanger model (usually LMTD). No information on exchanger thermal performance.	15, 25, 26
PHT heat transfer methods				
CIT or FIT	Coil or fuel inlet temperature	CIT	Primary measurement of CIT	27, 28
NFIT	Normalized FIT	T_{in}, T_{out}, $\dot{m}$ all HEXs	Calculation of fouling resistances for individual units and PTH model.	29
$Q_{furnace}$	Furnace heat duty	CIT, COT	Calculation of sensible heat.	7, 27
$FI_{tot} = (Q_{c,tot}-Q_{tot})/(Q_{c,tot}-Q_{f,tot})$	Network Fouling Index	T_{in}, T_{out}, $\dot{m}$ all HEXs	PHT network model.	30
Pressure drop methods				
ΔP	Pressure drop	Tube ΔP	Primary measurement	9
$\Delta P/\Delta P_c$	Hydraulic performance	Tube ΔP, $\dot{m}$	Requires hydraulic heat exchanger model. Normalization w.r.t. practical minimum.	19
C-factor	C-factor	Tube ΔP, $\dot{m}$	Based on primary measurements, simple calculation. No direct information on exchanger pressure drop.	25
PHT Pressure drop methods				
ΔP_{tot}	Pressure drop	Pressures	Pressure difference for entire PHT or sections	28, 31, 32

Such maximum occurs if the outlet temperature of the cold fluid reaches the inlet temperature of the hot fluid, which is unreachable in practice (an infinite heat exchange area would be required). With several simplifying assumptions, ε may be calculated as a ratio of temperature differences (*thermal effectiveness*) which requires only temperature measurements and very simple calculations. It is noted that the duty, and ε, may be different according to which stream (hot or cold) they are based on, and whether the temperature dependence of heat capacity is considered.

Alternatively, the exchanger performance can be defined as the ratio between measured duty and the predicted heat duty in clean conditions (Q/Q_c), which corresponds to a *practical* maximum. This indicator provides simultaneously the unit performance and the impact of fouling in a way easy to interpret. However, it requires measurements of flowrates and temperatures for all streams and, for variable conditions, a heat exchanger model to establish the clean duty performance.

The third category involves the calculation of the overall heat transfer coefficient (U) from measurements of temperature and flowrate and, typically, comparison with its corresponding value under clean conditions (U_c). U, or its normalized value with respect to U_c (often called *cleanliness factor*, *CF*) are commonly used to monitor fouling. However, the most popular fouling indicator used in industrial practice is, by far, the thermal fouling resistance, calculated as follows:

$$R_f = \frac{1}{U} - \frac{1}{U_c} \quad (1)$$

R_f , the additional resistance relative to a clean exchanger due to fouling, provides information on the fouling state of individual units and is (almost) independent of operating conditions. However, it does not provide direct information on the heat exchanger performance, and is often complemented by duty-based indicators (e.g. ref[20]). Refineries worldwide rely on classic R_f monitors (e.g. ref[37]), or updated versions[38, 39]. It should be noted that calculating R_f requires a model of the exchanger. This is typically based on simple LMTD and lumped models (i.e., average models that ignore any distribution within the exchanger). R_f and the standard calculation methods have been severely criticized. Takemoto *et al.*[40] highlighted that simplifying assumptions (e.g. on the evaluation of physical properties and heat transfer coefficients[41]) affect the estimation of R_f and, particularly, the apparent initial R_f often observed after cleaning. They showed that ignoring shell-side bypasses (heating fluid) leads to an over-estimation of

R_f, which can be misinterpreted by operators as sudden fouling deposition. Noise in the primary measurements (and especially in the flowrate) leads to scattering in the R_f time series. Crittenden *et al.*[42] showed that typical measurement errors may lead to errors in the order of 20% in R_f when using standard calculation methods. Improved calculation methods and models[22], smoothing techniques[8], or sophisticated filtering methods[43] have been applied in the attempt to reduce the scattering of calculated R_f series and facilitate the analysis. Coletti *et al.*[41] pointed out the inability of LMTD models of handling temperature cross of tube and shell-side outlet temperatures. Moreover, R_f calculations neglect the effect of flow constriction and roughness on the tube-side heat transfer coefficient. More recently, Diaz-Bejarano *et al.*[44, 45] showed that fouling resistance monitors are intrinsically unable to reflect the extent and properties of the deposit, and hence to discriminate between variations in deposit conductivity due to ageing or changes in fouling behaviour (e.g. deposition of inorganics) from deposit growth, suppression or removal processes. This can lead to highly misleading conclusions about the fouling state of an exchanger and wrong diagnosis of its causes.

At PHT level, the CIT (also called Furnace Inlet Temperature, FIT) and the furnace heat duty are the main direct thermal performance indicators used[7, 27, 28]. The FIT depends on the fouling state of all the individual units in the PHT and on the (variable) process conditions. A common approach is to calculate a Normalized Furnace Inlet Temperature (NFIT), dependent only on fouling build-up, by removing the fluctuations from process variability[28, 29, 46]. This normalization technique involves: i) evaluation of R_f over time for each unit in the PHT; ii) selection of standardized feed conditions (flowrate and temperature); iii) re-evaluation of the performance of the PHT and the NFIT by using i) and ii). The NFIT is then used to estimate the additional duty required to restore the initial NFIT (for a clean network) and the attached economic cost. A similar normalisation procedure will be sued later in this paper.

Negrão *et al.*[30] proposed a network index of fouling (based on the concept for single units by Jerónimo *et al.*[3]) using the total PHT heat duty in clean, pre-defined fouled, and measured conditions. The weight of each unit is calculated as the ratio of individual duty to the total PHT duty.

Pressure drop (ΔP) methods are usually based on tube-side pressure drop measurements, which depend on both the effect of fouling build-up and the variability in flowrate. This flowrate variability is

often substantial and may mask the underlying effect of fouling. To remove such effect, the exchanger hydraulic performance can be defined as the ratio between measured ΔP and predicted ΔP in clean conditions ($\Delta P/\Delta P_c$), for which suitable a hydraulic model is required. The application of this method has been limited to conceptual studies[19, 47]. Alternatively, Mohanty and Singru[25] proposed the use of a C-factor, from the analysis of flow through orifices, to provide a hydraulic fouling indicator independent of operating conditions. At the network level, the total pressure drop, together with the throughput, is a key indicator[28, 31, 32]. Good management of the pressure drop results in substantial economic benefits, by maintaining operation below the hydraulic limit (dictated by the capacity of the pump) or minimizing the loss in throughput when such limit is reached.

Finally, few publications in the literature address the interaction between hydraulic and thermal effects of fouling. Yeap *et al.*[19] assessed the performance of individual exchangers by plotting a thermal indicator (fouling Biot Number or ε) against $\Delta P/\Delta P_c$. This graphical representation was used in conceptual studies (e.g. to analyse the theoretical impact of the value of the deposit thermal-conductivity on the thermal and hydraulic performance of exchangers[48]), but does not appear to have been used for monitoring with actual plant data. Yeap *et al.*[19] also proposed a "Modified Temperature Field Plot" for heat exchanger network design purposes (rather than monitoring) by adding pressure drops to the original Temperature Field plot.

In industrial practice, monitoring of heat exchangers and fouling still relies on heat transfer methods and, in particular, on the classic description of the fouling deposit as a lumped thermal resistance R_f. Pressure drop in individual units are only rarely measured and monitoring of the properties of the deposit is almost unexplored. Monitoring tools that unambiguously and rapidly establish the time evolution of the thermal and hydraulic performance of an exchanger, and the extent and properties of the fouling deposit would be very desirable. They would greatly assist operators and engineers in assessing at a glance the performance of the exchangers, identifying critical ones and take appropriate and timely remedial actions. It is desirable to have as much of this information as possible on a single plot so as to easily visualize trends (current and predicted), the approach to operating limits, and ideally provide some diagnostic indication of the underlying causes of fouling.

In this paper, a novel model-based monitoring approach is presented, called the dynamic thermo-hydraulic TH-λ method (TH-λ method, pronounced TH-Lambda, for short), leading to an easy to use but highly informative monitoring visualisation (the TH-λ plot). The advantages of the novel analysis method and visualisation plot are demonstrated through several case studies, highlighting the differences from the traditional fouling resistance approach. The method and visualisation use advanced dynamic models and simulation framework, which are briefly introduced in Section "Models, their utilisation and Example Exchangers", for the analysis of plant data. After explaining the general features of the visualisation plot (Section "Dynamic thermo-hydraulic monitoring: TH-λ Plot"), several examples are illustrated with ideal (constant inlet) conditions (Section "Applications of the TH-λ Plot: Ideal examples"). In Section "TH-λ Plot with time-varying inlet conditions" the method is extended to deal with the time-varying inlet conditions occurring in industrial practice, by applying a normalization method. The use of the monitoring tool with actual plant data is demonstrated for an industrial case study in Section "TH-λ Plot with industrial refinery data", followed by a discussion and some concluding notes. This paper is an extended version of material presented in preliminary form in two separate conference papers[49, 50] and an oral presentation[65].

MODELS, THEIR UTILISATION AND EXAMPLE EXCHANGERS

As noted in the Introduction, most monitoring approaches in Table 1 make use directly or indirectly of some heat exchanger model (however simplified). The monitoring approach used here utilises the comprehensive set of models for shell-and-tube heat exchangers undergoing fouling in Hexxcell Studio™ [51]. These are based on i) the dynamic, distributed heat exchanger model by Coletti and Macchietto[52] which views exchangers as distributed in axial and radial directions; ii) the deposit and deposition formulation by Diaz-Bejarano *et al.*[53], which views deposit as multicomponent mixtures that can settle, react and be removed; and iii) the thermo-hydraulic analysis described by Diaz-Bejarano *et al.*[54], which utilises various simplifications of the deposit model and solution types, described in the following. The model equations are provided in references[44, 52, 53, 55, 56] and are summarised in Table 2.

Table 2. Main equations of modelling framework, adapted from ref.[55]

Heat Exchanger Model (Coletti and Macchietto [52])	
Tube-Side (Ω_t)	
Energy balance	$\frac{\partial\left(A_{t,n}(z)\rho_n(z)H_n(z)\right)}{\partial t} = -dir_n\frac{\partial\left(A_{t,n}(z)\rho_n(z)u_n(z)H_n(z)\right)}{\partial z} + p_n(z)h_n(z)(T_{l,n}\big\vert_{R_{flow,n}}(z) - T_n(z))$ $h_n(z)$ calculated by Sieder-Tate correlation[62]
Overall heat duty	$Q = \dot{m}\int_{T_{in}}^{T_{out}} C_p(T)dT$
Pressure drop	$\Delta P_{total} = \Delta P_{External} + \Delta P_{Headers} + \sum_{n=1}^{N_p}\left(P_{n,in} - P_{n,out}\right)$ $-\mathrm{dir}_n\frac{dP_n(z)}{dz} = \frac{C_f(z)\rho_n(z)u_n(z)^2}{R_{flow,n}(z)} = \frac{2\tau_{w,n}(z)}{R_{flow,n}(z)}$ $C_f = f(Re_n)$ (ref.[63])
Shell-side (Ω_s)	
Energy balance	$\frac{\partial(A_s\rho_s(z)H_s(z))}{\partial t} = -dir_s\frac{\partial(A_s\rho_s(z)u_s(z)H_s(z))}{\partial z} + \sum_{n=1}^{N_p} p_{s,n}h_s(z)(T_s(z) - T_{w,n}\big\vert_{r=RO}(z))$ $h_s(z)$ calculated with Bell-Delaware method [64]
Tube wall (Ω_w)	
Energy balance	$\rho_{w,n}C_{p,w,n}(z,r)\frac{\partial T_{w,n}(z,r)}{\partial t} = \frac{1}{r}\frac{\partial}{\partial r}\left(r\lambda_w\frac{\partial^2 T_{w,n}(z,r)}{\partial^2 r}\right)$
Deposit Model (Diaz-Bejarano *et al.* [53])	
Mass balance	$\left(\frac{\partial c_{l,i}(z,\tilde{r}_l)}{\partial t} - \frac{\tilde{r}_l}{\delta_l(z)}\dot{\delta}_l(z)\frac{\partial c_{l,i}(z,\tilde{r}_l)}{\partial \tilde{r}_l}\right) = \sum_{j=1}^{NR}\nu_{ij}r_j(z,\tilde{r}_l)$
Energy balance	$\rho_l(z,\tilde{r}_l)C_{p,l}(z,\tilde{r}_l)\left(\frac{\partial T_l(z,\tilde{r}_l)}{\partial t} - \frac{\tilde{r}_l}{\delta_l(z)}\dot{\delta}_l(z)\frac{\partial T_l(z,\tilde{r}_l)}{\partial \tilde{r}_l}\right)$ $= \frac{1}{\left(R_i - \tilde{r}_l\delta_l(z)\right)\delta_l(z)^2}\frac{\partial}{\partial \tilde{r}_l}\left((R_i - \tilde{r}_l\delta_l(z))\lambda_l(z,\tilde{r}_l)\frac{\partial T_l(z,\tilde{r}_l)}{\partial \tilde{r}_l}\right)$
Effective conductivity	$\lambda_{eff,n}(z) = \frac{q^{"}_{w,n}\big\vert_{r=R_i}(z)R_i\, ln\left(\frac{R_i}{R_{flow}(z)}\right)}{\left(T_{l,n}\big\vert_{r=R_{flow}}(z) - T_{l,n}\big\vert_{r=R_i}(z)\right)}$
Local Conductivity	$\lambda_{l,n}(z,r) = \sum_{i=1}^{NC} x_{l,i,n}(z,r)\lambda_i$
Prediction of rate of change in thickness (only used with Mode I)	
Overall rate of change	$\dot{\delta}_{l,n}(z) = (1 - b_{clean})\sum_{i}^{NC}\frac{1}{\rho_i}n_{f,i,n}(z) - \sum_{k=1}^{NCl} b_k\frac{1}{\rho_{l,n}(z,1)}n_{Cl,k,n}(z)$
Deposition rate[44]	$n_{f,i}(z)/\rho_i = p_i n_{ref}(z)/\rho_{gel}$ $n_{ref}(z) = \alpha' Re^{-0.66}Pr^{-0.33}\,exp\left(\frac{-E_f}{R_g T_{film}}\right) - \gamma'\tau_w$ (Ebert-Panchal functionality adopted [56])

In this paper, three configurations of the deposit model detailed in ref.[54] ("Modes") are used to generate and illustrate the TH-λ plot (Mode III is not used here):

a) Mode I – Distributed, multi-component deposit: the deposit is described by local mass and heat balances, multiple fouling species, chemical reactions (if any) and deposition (or removal) mass fluxes at the surface. Its purpose is to accurately predict the build-up of fouling.

b) Mode II – Uniform deposit: a simplification of Mode I featuring uniform deposit thickness and conductivity throughout the exchanger. Its purpose is to infer the apparent amount and

characteristics of fouling from measurements or quantify the impact of ideal fouling deposits on the exchanger performance.

c) Mode IV – Clean exchanger: a further simplification of Mode I that neglects the presence of the deposit altogether. Its purpose is to estimate the pressure drop and heat duty of the unit in clean conditions for given inlet conditions.

Furthermore, two solution types are used:

i) Analysis type (A): measured inlet and outlet conditions (temperature, flowrate and pressure drop) are used as inputs to calculate the fouling deposit characteristics (thickness and conductivity).

ii) Prediction type (P): inlet conditions and deposit characteristics are used to calculate the heat duty (hence outlet temperatures) and pressure drop of the heat exchanger. The deposit characteristics direct inputs or given over time by a deposition rate model.

To simplify the nomenclature in the following, the deposit configuration and solution type used at each stage are labelled by the deposit mode plus the solution type acronym. For example, Mode II-P means the use of a Mode II deposit solved in Prediction type.

Heat Exchangers used in the Examples

Two heat exchangers from two different refineries are used in the examples presented in this paper, E05AB and E0155AB. Details on the geometries and operating conditions of these units are provided in ref.[54] and ref.[55], respectively.

Heat exchanger E05AB is used in some idealised examples. Fouling in this heat exchanger was studied in detail in a previous publication[54]. The measured inlet temperatures and flowrates of both hot and cold streams for this unit over a thousand days of operation, divided into 3 periods, are shown in Figure 1. Pressure drops were not measured but are calculated using the heat exchanger model as a soft-sensor. First, constant inlet conditions of temperature and flowrate are used to illustrate the features of the novel method and visualisation in Sections 3 and 4. These constant inlet conditions correspond to the averages of the historical data for E05AB in operating Periods 1 and 2 (Figure 1). The performance of E05AB under fouling is simulated with Mode I-P (full deposition) model, using the fouling (α, γ, and

E_f) and ageing (A_a) parameters in Table 3 (these parameters were fitted to plant data[54]). In the absence of information on the nature of the deposit, an organic fouling deposit was assumed. Parameter Set B is used here unless stated otherwise.

Heat exchanger E155AB is used to illustrate the full application of the TH-λ Plot in an industrial refinery case study. In this case all temperatures, flowrates and pressure drop measurements were available. A detailed analysis of the fouling state in this exchanger over the same operating period used here is provided in ref.[55].

Table 3. Fouling and ageing parameters of E05AB[54]

Set	A_a (s^{-1})	E_f (kJ mol^{-1})	α' (kg $m^{-2}s^{-1}$)	$10^9\gamma'$ (kg $m^{-2}s^{-1}Pa^{-1}$)
A	0	28.5	1.32	15.5
B	0.0015	28.5	1.00	3.6
D	0.005	28.5	1.20	1.2

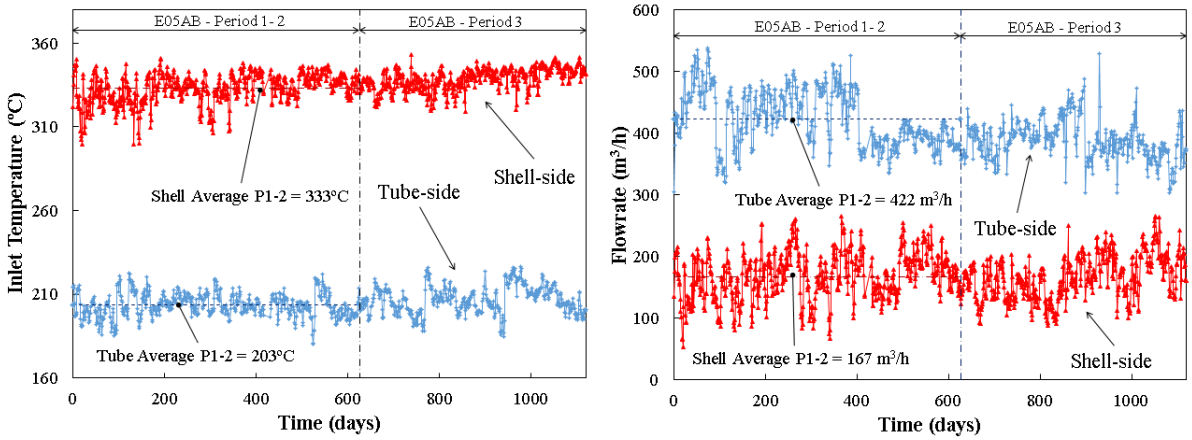

(a) (b)

Figure 1. Measured inlet temperatures (a) and flowrates (b) to E05AB.

DYNAMIC THERMO-HYDRAULIC MONITORING: TH-λ PLOT

The TH-λ plot is constructed to monitor the performance of a heat exchanger using the following indicators:

1) Thermal indicator: Fouled-to-clean heat duty ratio ($Q(t)/Q_c$).
2) Hydraulic indicator: Fouled-to-clean tube-side pressure drop ratio ($\Delta P(t)/\Delta P_c$).
3) Temporal indicator: Points at various intervals (here monthly) are labelled to show its time evolution. More frequent data point labelling, using actual dates as label, could be used.

The plot has the exchanger hydraulic performance ($\Delta P(t)/\Delta P_c$) on the X axis and the thermal performance ($Q(t)/Q_c$) on the Y axis. An example is shown in Figure 2(a), where a performance line, named *TH-line* (continuous line) is shown for 9 months of operation, starting from a clean state (for which thermal and hydraulic indicators equal 1). As noted, establishing the performance *in clean conditions* (Q_c, ΔP_c) requires a model. This has been calculated using a Mode IV-P (no deposition) model. The performance *under fouling* would be obtained in practice from plant measurements of inlet and outlet temperatures, flowrates, and tube-side pressure drop (as shown later). Here, for illustration purposes, it has been simulated considering constant inlet conditions to E05AB and using a Mode I-P.

The thermal and hydraulic performance relative to clean conditions are given simultaneously by each point along the TH-line. The distance between successive time points reflects how fast the relative change is happening. The net deposition (or removal) of fouling material results in an increase (or decrease) in deposit thickness, and hence pressure drop, which is reflected as a displacement in the X (hydraulic) axis. Changes in the heat exchanged are reflected as a displacement in the Y (thermal) axis. The latter may be due to: i) change in deposit thickness; ii) change in the conductivity of the deposit due to internal transformations (e.g. ageing); iii) change in the conductivity of the deposit due to foulant composition changes (hence the λ in the TH-λ name).

The TH-λ plot becomes even more useful when monitored data and trends are complemented with some additional reference lines of practical interest:

a) Thermal and hydraulic limit lines, TL and HL (dashed lines in Figure 2a).

Useful limit lines refer to minimum acceptable performance and may be operational constraints (e.g. maximum allowable pressure drop) or design targets (e.g. minimum heat duty). In Figure 2(a), the hydraulic limit (HL), indicated by the vertical line, was set at 5 times the value of the clean pressure drops (as recommended in ref.[19]), whilst the thermal limit (TL), indicated by the horizontal line, was set to a minimum thermal performance of 30% of the clean one, as recommended by Zabiri *et al.*[57]. These limits are typically set by engineering personnel. By comparing the location and evolution of the TH-line relative to the TL and HL, one can immediately obtain useful insights into the dominant impact of fouling (hydraulic or thermal).

b) Reference conductivity lines, named *λ-lines* (dotted lines in Figure 2b).

The thermal performance is linked to the hydraulic one by the thickness of the deposit as it grows (or is removed) and its thermal-conductivity (both of which may change over time both axially and radially). As a result, *if a suitable thermo-hydraulic model of the exchanger is available*, it is possible to calculate and plot the evolution of the thermal-hydraulic performance for a growing deposit with fixed conductivity and inlet conditions, i.e. a reference conductivity line or *λ-line*. Here, these were calculated using a Mode II-P (uniform deposit) model. For organic fouling, for instance, the calculated lines for gel (fresh deposit, with λ = 0.2 W m^{-1} K^{-1}), completely coked deposits (λ = 1.0 W m^{-1} K^{-1}) and some intermediate values are shown in Figure 2(b). The gel and coke lines delimit the area of expected performance of the exchanger with organic crude oil fouling. By comparing the location and evolution of the TH-line relative to the reference λ-lines, one can obtain valuable insights into the likely conductivity and nature of the deposit and its evolution. The conductivity of the TH-line used for this comparison is the *apparent* conductivity of the deposit (*apparent* - indicated with subscript *a* - as it includes the overall contribution of a spatially distributed, potentially heterogeneous deposit[54]). In the example, the TH-line gradually moves away from the gel reference line towards the coke line, indicating deposit ageing. The apparent conductivity of the deposit is nearly 0.4 $Wm^{-1}K^{-1}$ at the end of the year. It should be noted that the location of the λ-lines will depend on the geometry of the heat exchanger, physical properties of the fluids, and inlet conditions of temperature and flowrate. In addition, the use of the λ-lines as described here is limited to cases where the contribution of shell-side fouling to the overall thermal performance is negligible. This is the most common case in refinery heat exchangers[52].

Finally, a Predicted TH-line (PTH-line) can be optionally included as a reference for the predicted (future) decay in heat exchanger thermo-hydraulic performance (as opposed to the monitored decay based on past and current measurements). The PTH-line is generated with predictive fouling models previously fitted to past plant data (e.g. refs.[52, 54]). Such line has two purposes: i) to provide an indication of the expected future performance; ii) to highlight unexpected changes in fouling behaviour, by comparing the TH-line from measurements to the Predicted TH-line at a given time.

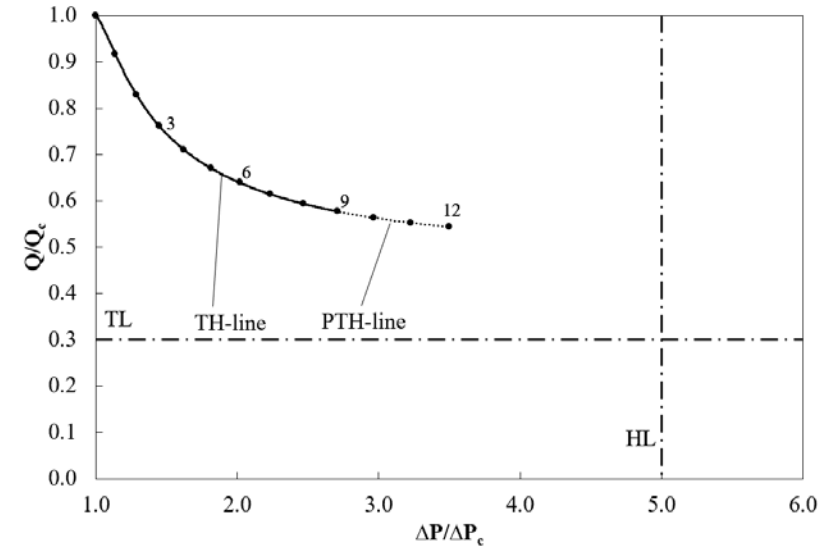

(a)

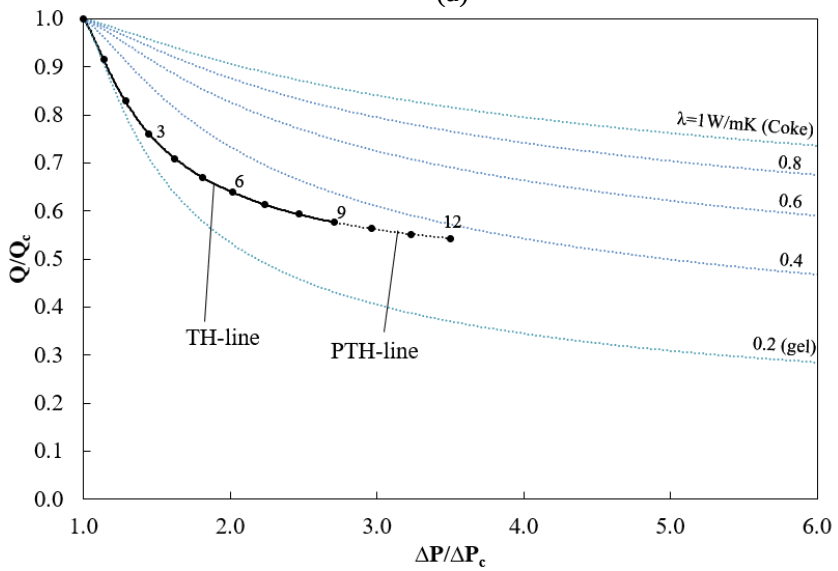

(b)

Figure 2. TH-λ Plot with TH-line, PTH-line and operating limit lines (a) and λ-lines within organic limits (b). The dots of the TH-line indicate months of operation after cleaning.

APPLICATIONS OF THE TH-λ PLOT: IDEAL EXAMPLES

In this section, several applications of the novel graphical approach are illustrated by means of examples produced by simulation with constant inlet conditions. Heat exchanger E05AB is considered in all cases with the same configuration as in Section "Dynamic thermo-hydraulic monitoring: TH-λ Plot", unless stated otherwise.

Organic fouling: Identification of underlying phenomena

The behaviour of a heat exchanger undergoing fouling depends on the relative values of deposition and ageing rates. Traditional monitoring techniques (e.g. R_f-based method) are inherently unable to discriminate between these phenomena. For instance, consider the three fouling resistance curves in Figure 3(a) that correspond to the thermo-hydraulic behaviour of the E05AB for three sets of fouling parameters estimated from the same set of plant data but considering three different ageing rates[54] (A, B, D in Table 3). The fouling resistances profiles calculated with all these sets are very similar. If this metric is used in isolation, these results would be interpreted as the effect of similar deposition rates in all three cases.

The TH-λ plot for the same 12 months data (Figure 3b) shows quite different TH-lines with parameter Sets A, B and D. Some more informative conclusions can be extracted straight away: i) the net deposition rate is quite different (Set A < B < D) as evidenced by a faster increase in ΔP for Cases B and D; ii) with Set A, the TH-line follows the lower limit for organic fouling (gel λ-line), and therefore the deposit does not age; iii) with Set B and D, a pronounced deposit ageing effect is evidenced (stronger in D than B) which significantly attenuates the thermal losses of fouling; iv) by extrapolating the trends, with Set A the TL and HL are expected to be reached at approximately the same time, while with Set B the HL is expected to be reached before the TL; with Set D the HL is reached much more quickly, after 10 months.

The R_f-based monitoring may be misinterpreted as it does not evidence ageing effects, whilst the proposed TH-λ representation helps to correctly identify the underlying phenomena and select appropriate mitigating decisions.

As discussed in ref.[54], although the conductivity of the organic deposit may reach locally (near the wall) values close to that of coke (1 $Wm^{-1}K^{-1}$), the apparent conductivity of organic deposits (as a whole) is unlikely to reach values above 0.4 - 0.6 $Wm^{-1}K^{-1}$. Therefore, a value of 0.6 $Wm^{-1}K^{-1}$ can be considered as the *practical* limit for an organic deposit. This aspect is important when considering multi-component deposits, discussed later in this paper.

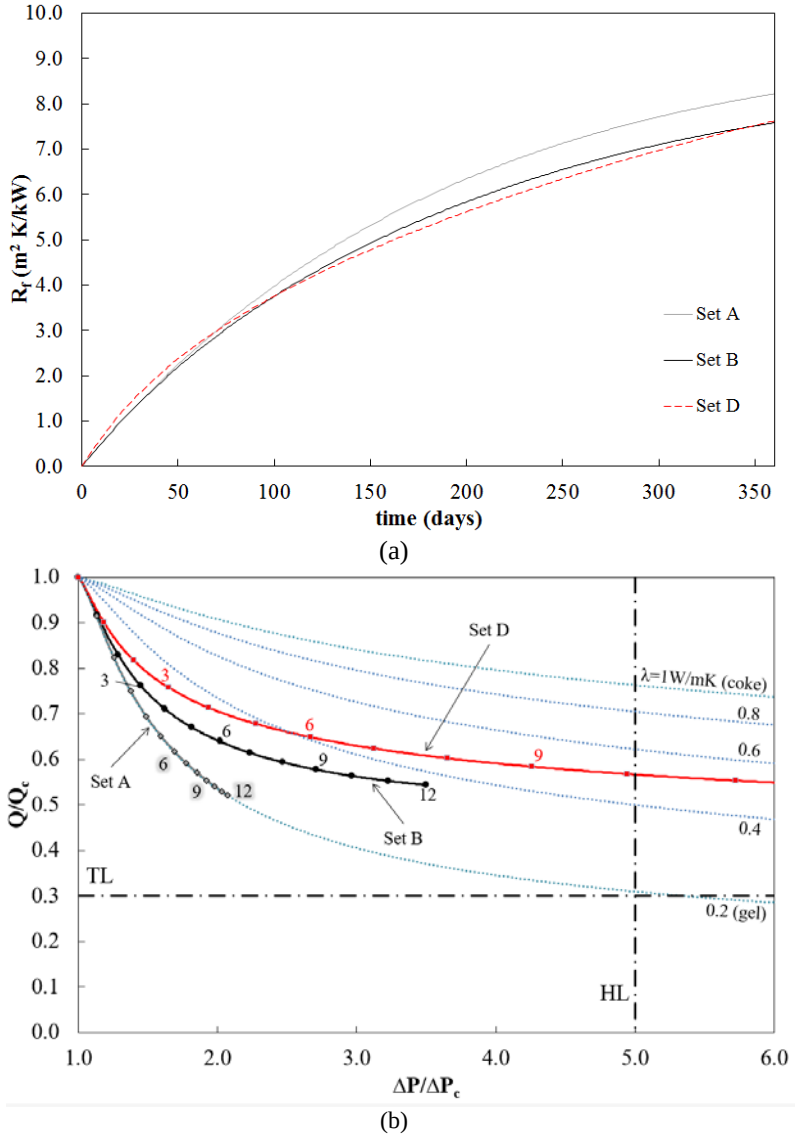

Figure 3. Fouling resistances over time (a) and TH-λ Plot (b) for three cases with different ageing rates.

Assessment of cleaning effectiveness

The TH-λ plot also provides valuable information on the effect of cleaning actions. As an example, a partial cleaning of the same exchanger E05AB is considered. The operation sequence, based on a real operation sequence[54], includes a first operation period of 349 days (Period 1, P1), a partial cleaning, and a second operation period of 268 days (Period 2). Here, the simulation was performed for the same schedule, ageing and fouling parameters (Set B), and cleaning effectiveness, but with the constant flow and temperature inputs indicated in Figure 1. With a R_f-based monitoring method (Figure 4a) the cleaning action is shown as a sudden decrease of 40% in resistance, indicating an improvement in thermal performance after the cleaning. However, the impact of this reduction on heat duty is not directly provided by the graph. Furthermore, no insight is provided into the thickness, thermal-conductivity and composition of the remaining deposit, nor, operationally more important, on the hydraulic effects of the cleaning.

In the TH-λ Plot (Figure 4b), on the other hand, the last point on the TH-line before (indicated as *cleaning*) and the first point after cleaning (indicated as *operation re-start*) give clear information about: i) the improvement in thermal performance (here duty increased from 55% to 70% of the clean value); ii) the decrease in pressure drop (here from 3.4 to 2.4 times the clean pressure drop), which gives an indirect estimate of the amount of deposit material that has been removed; iii) through the closeness to the reference λ-lines, insight into the (apparent) degree of coking of the deposit not removed by the particular cleaning method. Here, the results indicate that a top low-conductive layer was removed (probably organic gel-like), but older deposit with significant degree of coking was not. A more detailed analysis to extract information on the local degree of coking was presented in ref.[54].

Partial removal of the layer due to high shear stress may occur if the flowrate varies[10, 45]. For this type of removal to be detected, as explained for a partial cleaning, it is necessary to decouple the effect of time-varying inlet conditions on the performance indicators from that of fouling, as discussed later in this paper.

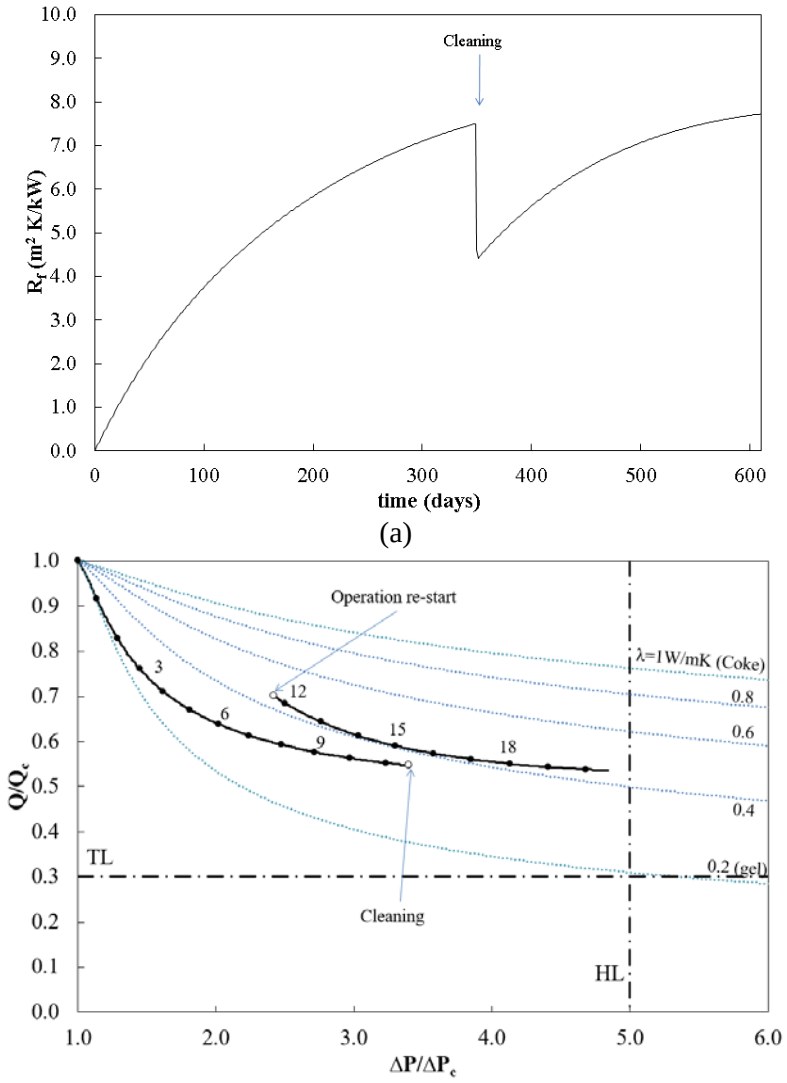

Figure 4. Performance of the exchanger undergoing fouling, including a partial cleaning after 346 days: (a) Fouling resistances over time; (b) TH-λ Plot.

Multi-component deposits: Uniform organic/inorganic mixture

Inorganic salts generally have greater thermal conductivity than organic deposits, and their presence leads to fouling deposits with less negative impact on thermal performance. The thermo-hydraulic impact of binary organic/inorganic mixtures was studied for a single tube with uniform wall temperature heating by Diaz-Bejarano *et al.*[44]. Here, an example for a heat exchanger is used to illustrate the how the presence of inorganics is reflected in the TH-λ plot. The reader is referred to ref.[44] for details on the approach used to simulated mixed organic-inorganic deposition.

In the example, the deposit layer is formed by deposition of: a) organic matter, represented as a binary mixture of gel and coke, as in previous examples; b) Fe_3O_4, with a conductivity 3 times that of coke; c) FeS, with a conductivity 5 times that of coke[58, 59]. The parameter Set B is assumed for the organic deposition rate. The deposition rates of Fe_3O_4 and FeS are assumed to be 30_{vol}% and 70_{vol}% of the deposition rate of gel, respectively. The results are compared to the base case with organic fouling only, discussed in Section "Dynamic thermo-hydraulic monitoring: TH-λ Plot".

The total fouling resistance is plotted in Figure 5(a). R_f grows faster in the organic than in the organic/inorganic case. After a year, R_f for the organic deposition case is more than three times that of organic/inorganic mixture. However, if a thermal performance measure, such as R_f (Figure 5a), is considered in isolation, one may erroneously conclude that deposition is faster in the organic than in organic/inorganic case, while the opposite is true.

The TH-λ Plot is used to visualize the thermo-hydraulic performance of the heat exchanger (Figure 5b). For organic matter, as the deposit ages, the TH-line gradually moves from the gel λ-line towards the coke λ-line. At the beginning, there is a fast decrease of the thermal performance from a completely clean state 1 to Q/Q_c = 0.75 in just three months (i.e. 25% performance loss). In the months that follow, the thermal performance continues decreasing albeit at a lower rate. On the other hand, the pressure drop increases very fast. This is observed as a gradually increasing distance between the monthly black points in the X direction of the plot.

In the presence of inorganics, the thermal performance is always higher than that indicated by the coke λ-line. However, this does not imply slower deposition. In fact, the hydraulic performance reveals a very fast build-up of fouling: the pressure drop doubles with respect to clean conditions in just 3 months; that is, half the time compared to the organic case. Figure 5(b) clearly shows that deposition of organic material in isolation mainly affects the thermal performance, whilst deposition in combination with inorganics may shift the main impact of fouling to the exchanger's hydraulics.

The underlying causes behind such behaviour may be explained by the evolution and properties of the deposit layer, for which the reader is referred to previous publications[44, 60].

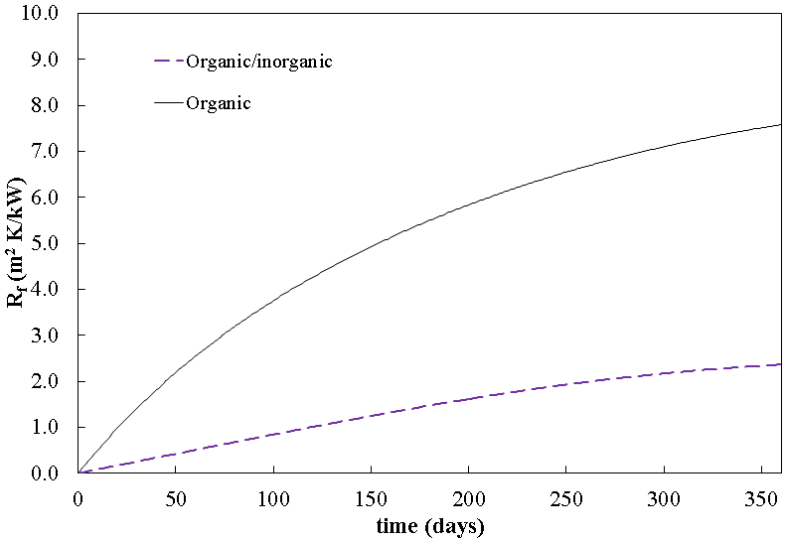

(a)

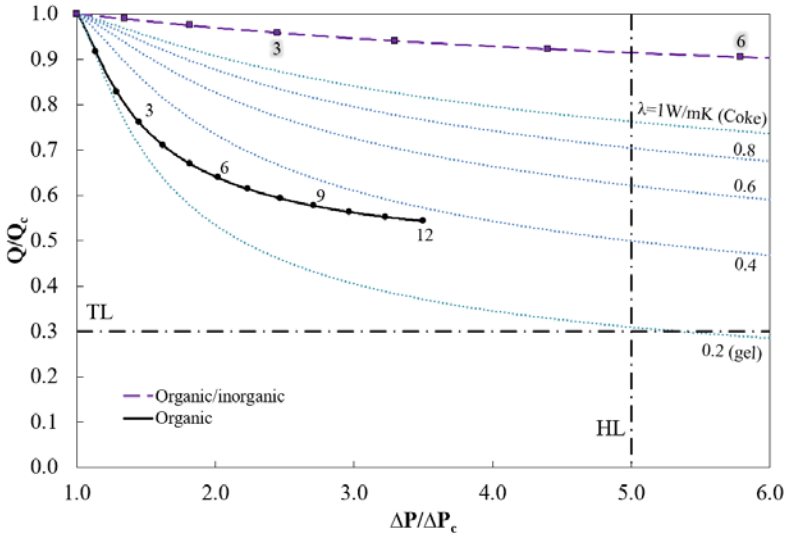

(b)

Figure 5. Performance of the exchanger undergoing organic fouling and mixed organic-inorganic fouling: (a) Fouling resistances over time; (b) TH-λ Plot.

Detection of deviations in fouling behaviour

Most current practices not only fail to regularly measure and monitor the hydraulic performance, but also have limited ability to detect changes in fouling behaviour. As discussed in ref.[44], deviations from the expected behaviour due to acute organic fouling or presence of inorganics can be potentially

detected and diagnosed only if thermal and hydraulic measurements are used in combination. The capabilities of the new plot to highlight such changes are discussed in this section.

It is assumed that the heat exchanger, in normal circumstances, undergoes organic deposition (as in the base case, Section "Dynamic thermo-hydraulic monitoring: TH-λ Plot"). After 6 months (180 days) an event somewhere upstream leads to a change in fouling behaviour in E05AB. Two examples of plant upset are considered: a) deviation due to acute organic fouling; b) deviation due to inorganic fouling (e.g. resulting from upstream corrosion).

The organic deposition model, fitted to past plant data, is used at month 6 to predict the thermo-hydraulic behaviour of the unit (PTH-line) for the next 6 months, up to month 12. It is shown that the abnormal behaviour may be detected by comparing the predicted fouling behaviour to the actual performance indicators from plant measurements (TH-line).

Deviation due to acute organic fouling

The first case assumes a change in oil blend or type of oil being processed (e.g. from conventional oil to a high fouling propensity oil such as slag or heavy oil) leading to acute organic fouling. The composition of the fresh deposit remains unchanged (only gel), but the fouling rate becomes twice as fast. The R_f-based monitoring method (Figure 6a) shows a sudden increase in the fouling resistance after the event. A change in behaviour is detected, but no information is provided about the hydraulic impact, which may be relevant due to the fast build-up of material.

In the TH-λ plot (Figure 6b), the performance of E155AB at month 6 is given by the TH-line (as in previous examples). The PTH-line, predicted at month 6 (also shown in Figure 6b) shows that by month 12 a decreasing duty is expected to about 54% of clean duty, a pressure drop increase to 3.5 times the clean value, and a deposit with coking to approximately $\lambda = 0.4$ W m^{-1} K^{-1}. Compared to this predicted behaviour, the TH-line starts to deviate already from month 7, with a larger deviation detected by month 8. The change in behaviour is evidenced as a much larger increase in pressure drop than expected. This, together with a deviation from the PTH-line towards lower values of thermal efficiency, indicates that the additional foulant has low conductivity and is most likely organic in nature. The fast deposition of low conductive material has a greater weight on the thermal impact of fouling than the also ongoing

ageing process. This explains the lower thermal efficiency compared to the predicted trend. After 10 months, the exchanger performance approaches the hydraulic limit. Therefore, although the R_f-based method shows a deviation, the TH-λ plot provides much more complete and useful information as to its causes and effects.

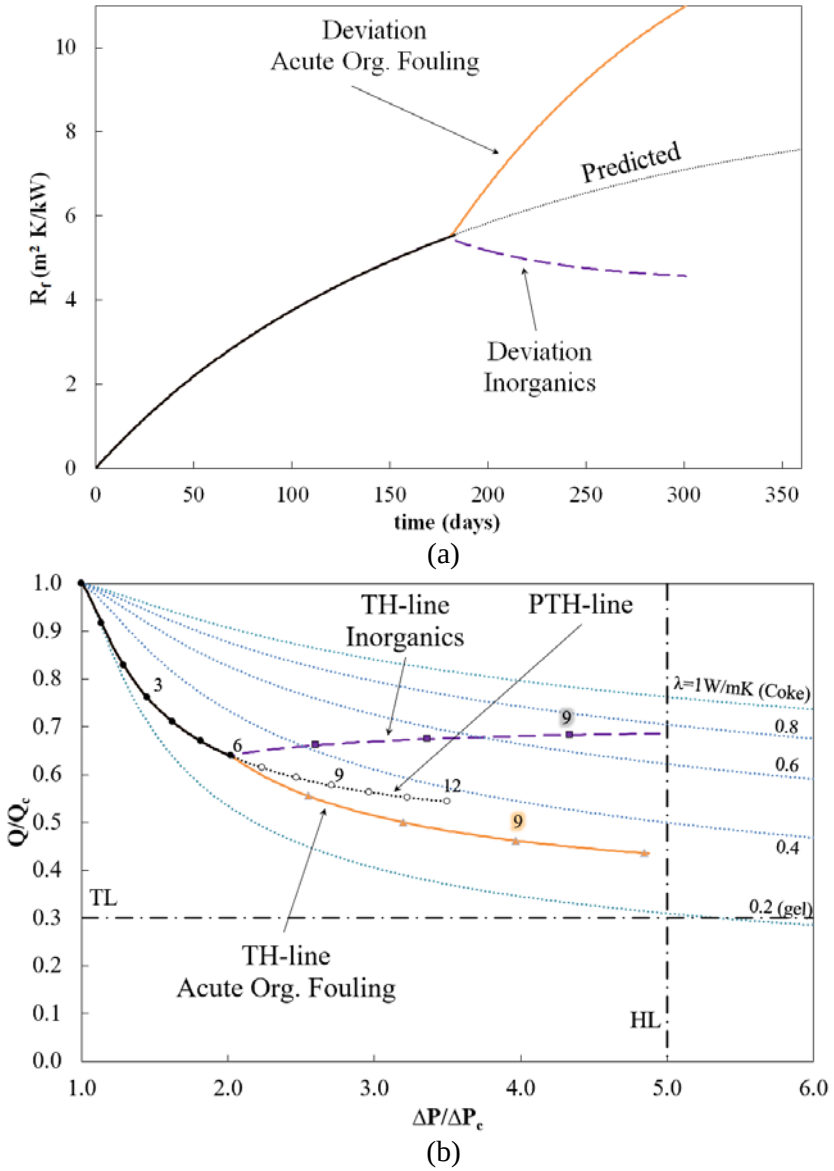

Figure 6. Performance of the exchanger undergoing fouling for a change in behaviour after 6 months: (a) Fouling resistances over time; (b) TH-λ Plot.

Deviation due to inorganic fouling

In this second case, an inorganic material is assumed to start depositing after 6 months in addition to the usual organic fouling. As in Section “Multi-component deposits: Uniform organic/inorganic

mixture", a mixture of Fe_3O_4 and FeS is considered to deposit. After the onset of the event the total deposition rate is doubled, and the fresh deposit contains 50% of organic gel and 50% of inorganics. In this case, the R_f-based method completely fails to detect the change in underlying behaviour (Figure 6a). In fact, it indicates that fouling becomes less severe than predicted, which is incorrect and could potentially lead to erroneous interpretation and mitigation or cleaning decisions.

In the TH-λ plot (Figure 6b), a change in behaviour is evidenced, as before, by a higher and much faster increase in pressure drop compared to the predicted trend (the hydraulic limit is reached before 10 months of operation). Now, however, the deviation of the TH-line towards greater thermal efficiency also indicates that the new foulant is highly conductive and, probably, of inorganic nature. The TH-line tends to but does not reach the reference coke λ-line. However, it does cross the 0.6 $Wm^{-1}K^{-1}$ λ-line, previously defined as the practical organic upper limit, which provides a solid indication of enhanced conductivity due to inorganics.

TH-λ PLOT WITH TIME-VARYING INLET CONDITIONS

So far, the use of the TH-λ plot has been illustrated with Q and ΔP generated from simulations with fixed inlet conditions (temperature and mass flowrates of hot and cold fluids) to a detailed exchanger model and estimated fouling parameters. In these conditions, the Q/Q_c and $\Delta P/\Delta P_c$ ratios are monotonic functions of time (the former decreasing, the later increasing), leading to smooth TH-lines.

With actual plant data that ideal scenario is unlikely. Heat duty is calculated from measured flowrate and inlet and outlet temperatures of the hot and cold fluids, and pressure drop can be measured directly. In both cases Q/Q_c and $\Delta P/\Delta P_c$ will present fluctuations as a consequence of: a) variability in process conditions (inlet temperatures and flowrates); b) measurement errors; and c) changes in underlying fouling behaviour other than due to net deposit growth (e.g. partial removal, changes in composition, ageing).

In this section a first step towards the systematic use of the TH-λ method with plant data is presented by considering time-varying inlet conditions (item a) above). For illustration purposes, instead of using Q and ΔP from measurements, these are generated from simulation with a Mode I-P deposit model as a function of time-varying inlet conditions. This allows focusing the discussion on the fluctuations

derived from process variability in a TH-line that is unaffected by measurement error (item b). E05AB is used again as example with the actual measured inlet temperatures and flowrates over the entire Period 3 in Figure 1.

Variability in inlet conditions and generation of TH-line

The measured inlet conditions to E05AB for Periods 1 to 3 are shown in Figure 1. Significant variability is observed: inlet tube and shell-side temperatures vary in a range of 30ºC and 50ºC, respectively, while flowrates vary in a range of about 200 m^3/h.

With varying inlet conditions, the generation of the TH-line is performed in the same way as with constant inputs, that is, by simply dividing the fouled duty and pressure drop by the corresponding predictions in clean conditions. The TH-line thus generated is shown in Figure 7. The thermal performance shown in the figure is the result of the contribution of fouling and inlet variability. Whilst the former is responsible for the overall decay over time, the latter reflects significant short-term changes in the performance that may mask more subtle effects such as changes in fouling behaviour. For instance, seven months after the start of Period 3 (around day 840), when the unit is already heavily fouled, Q/Q_c varies between 45% and 70% just as a result of variability in the inlet conditions. Q/Q_c (Y-axis) fluctuates over time as a consequence of the different sensitivity of Q and Q_c to changes in the inlet temperatures and flowrates. Inlet conditions that maximize the temperature difference between hot and cold fluids (low cold fluid temperature, high hot fluid temperature, and high flowrates) lead to lower values of Q/Q_c and vice versa. $\Delta P/\Delta P_c$ however is less affected by process variability and shows a monotonic rising trend over time (indicating positive net deposit growth). In order to apply some of the concepts in Section “Applications of the TH-λ Plot: Ideal examples”, it is useful to decouple these two effects. A methodology is proposed below.

Normalization method to remove process variability

The following methodology is proposed to normalize the thermo-hydraulic behaviour (TH-line) to that achieved under pre-defined *reference* working conditions, in order to remove process variability:

1) Collection of time sequences of Q and ΔP data obtained from plant measurements.

2) Generation of time series of apparent deposit characteristics, λ_a and δ_a by feeding Q and ΔP to a Mode II-A model.

a) If the measurement noise is significant it propagates to the λ_a and δ_a time series. In such case a smoothing of the λ_a and δ_a time series should be performed as an intermediate step by applying, for instance, a centred moving average.

b) In such case, by calculating the difference between the values of Q and ΔP before and after smoothing, it is possible to generate error bars to display together with the smoothed TH-line, for completeness. The error bars are calculated as twice the standard deviation.

3) Selection of reference fixed inlet conditions.

4) Values from 2) and 3) are fed to a Mode II-P model to generate the (normalized) fouled Q and ΔP time profiles.

5) Computation of Q_c and ΔP_c over time using the fixed inputs to a Mode IV-P model.

6) Results of steps 4) and 5) are used to produce a Normalized TH-line, that is, a NTH-line.

Normalized TH-lines and Range of Operation

The selection of appropriate *reference* conditions for the generation of the NTH-line is essential to obtain a performance line that, without the process variability, still represents adequately the time-variation of the performance of the exchanger as fouling builds up.

Here, it is proposed to choose the reference inlet conditions around those at which the operation is desired, which we call *nominal* operating conditions. If past historical data is available (as for E05AB), those can be used to extract the nominal point. As shown in Figure 1, the inlet conditions fluctuate around an average value (dotted lines). This is probably the result of process control trying to operate the exchanger at some desired steady-state operating conditions. Consequently, the average values are chosen as the nominal point, and those conditions are assumed to apply to the period being monitored. If no past plant data was available, this information would be provided by a process/control engineer. In fact, a nominal point chosen based on historical data should always be double-checked by a process engineer, as those conditions should be representative of how the plant is operating currently and of

how the plant is going to operate in the future. This is crucial to use the TH-λ Plot not only as a monitoring tool, but particularly if predictive PTH-lines are to be included.

For the example in this section (E05AB), the *nominal operation* was taken as the average values of inlet temperatures and flowrates in Periods 1 and 2, indicated in Figure 1. By applying the normalization method, a smooth NTH-line is obtained, shown in Figure 7. At each time, the apparent conductivity and thickness are calculated from the measurements with a Mode II-A model, reflecting all previous history (including process variability). These are fed to a Mode II-P model in order to re-evaluate the thermo-hydraulic performance of the heat exchanger with such fouling deposit inside the tubes, but operating under reference inlet conditions, leading to the NTH-line. As a result, the NTH-line presents small fluctuations which are result of the variation of the fouling rate over time, as the local conditions of temperature and velocity (hence deposition rate and shear stress) depend on the actual time-varying conditions in the exchanger. The TH-line fluctuates around the corresponding NTH-line. This indicates that the reference conditions used to generate the NTH-line are indeed representative of the past and current operation of the unit.

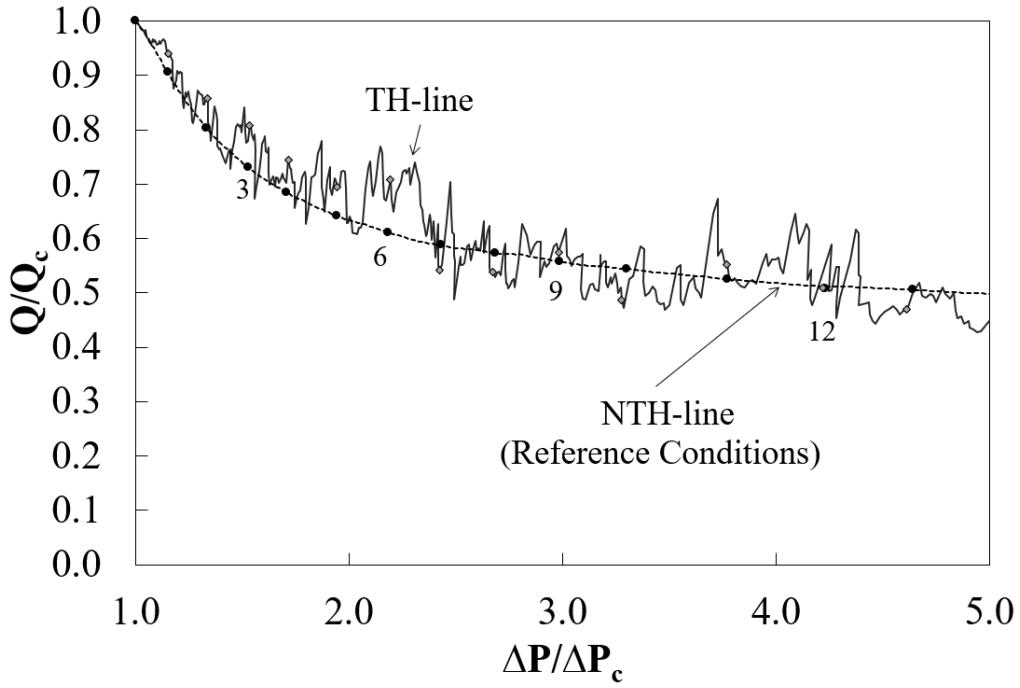

Figure 7. Simulated decay in Performance due to fouling in E05AB - Period 3: TH-line obtained with time-varying inputs and the corresponding NTH-line obtained with Nominal inlet conditions for E05AB.

As discussed earlier, the fluctuations in Q/Q_c are explained mainly by the variability in the inlet conditions. Since the relative position of the TH-line and the NTH-line depends on the reference conditions selected, the normalization methodology provides an opportunity to study the range of operation of the unit on the TH space. Based on recorded historical data (in the example, data from Periods 1 and 2), the following sets of reference inlet conditions can be defined, in addition to the Nominal operation:

a) ***Maximum driving force*** (*MaxDF)*: the combination of expected maximum $T_{in,s}$, maximum tube flowrate, maximum shell flowrate and minimum $T_{in,t}$ (based on past data) that result in a maximum temperature driving force in the exchanger and, consequently, minimum Q/Q_c.

b) ***Minimum driving force*** (*MinDF*): the combination of expected minimum $T_{in,s}$, minimum tube flowrate, minimum shell flowrate and maximum $T_{in,t}$ that result in a minimum temperature driving force in the exchanger and, consequently, maximum Q/Q_c.

By applying the normalization method in the previous section, it is possible to generate two additional NTH-lines for these reference operating conditions. The resulting reference lines provide useful information on the TH range of operation, as illustrated in the plot in Figure 8. The area between the *maximum* and *minimum* driving force lines (MinDF, MaxDF) includes all possible scenarios based on the recorded variation in inlet conditions, i.e. the expected operating band for the typical fouling behaviour in the unit. This area provides the engineer with the maximum and minimum performance achievable by modifying the inlet conditions as the heat exchanger fouls. As shown in Figure 8, the maximum and minimum lines provide a very conservative estimation of the operating band (i.e. it is very wide). It is quite unlikely that all 4 inlet conditions that lead to either maximum or minimum driving force happen simultaneously, and as a result the lines are rather far from the TH-line. Alternatively (or additionally), one may consider maximum and minimum operating lines based on some probability of the limiting inlet conditions occurring, i.e. establish a degree of confidence based on the variability of each measurement:

a) *Maximum driving force line with 95% confidence* (MaxDF95%, lower limit for Q/Q_c): combination of $T_{s,in} + 2\sigma_{T_{s,in}}$, $\dot{m}_t + 2\sigma_{m_t}$, and $\dot{m}_s + 2\sigma_{m_s}$ and $T_{t,in} - 2\sigma_{T_{t,in}}$.

b) *Minimum driving force line with 95% confidence* (MinDF95%, higher limit for Q/Q_c): combination of $T_{s,in} - 2\sigma_{T_{s,in}}$, $\dot{m}_t - 2\sigma_{m_t}$, and $\dot{m}_s - 2\sigma_{m_s}$ and $T_{t,in} + 2\sigma_{T_{t,in}}$.

For the case study analysed (Figure 8), the maximum and minimum driving force NTH-lines with 95% confidence (MinDF95% and MaxDF95%) seem to better capture the fluctuations in performance observed as a result of process variability.

In practice, this first step may be used to analyse the variability in the thermal performance under fouled conditions that can be expected for the unit. This is useful not only for monitoring but also for control. The analysis may be used to predict which operation limit is likely to be hit first under different operating conditions and to evaluate the energy losses due to fouling. In this context, λ-lines cannot be included, since their location depend on the inlet conditions and represent fixed references only when those conditions are constant.

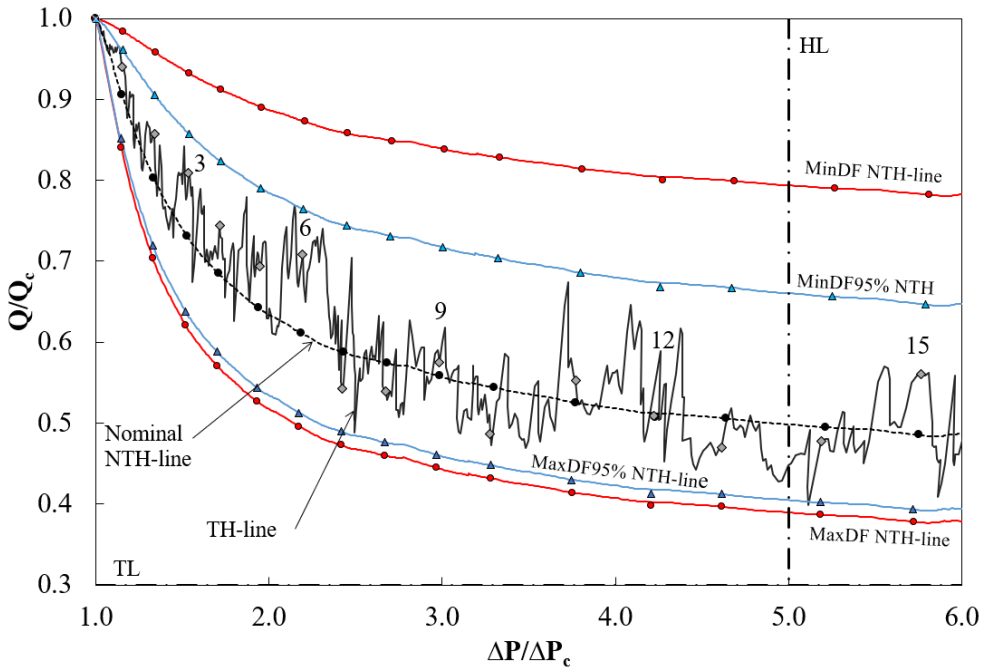

Figure 8. TH-line and several NTH-lines for Nominal Point, Overall MaxDF and MinDF, and max and min DF with 95% confidence, for E05AB-P3.

TH-λ Plot under time-varying inlet conditions after normalization

Returning to the main point of the paper, the normalization method presented allows removing the effect of inlet condition variability on the exchanger performance. Once the Nominal point is selected,

λ-lines consistent with the NTH-line can be generated to assess the impact of fouling on the thermal and hydraulic performance independently from fluctuations in the inlet conditions. This dynamic normalization procedure provides a basis for identification of exchangers more adversely affected by fouling and thus requiring cleaning or even a retrofit or re-design. It is also possible to plot reference λ-lines for the nominal inlet conditions. As a result, a full TH-λ Plot can now be generated and the analysis of fouling behaviour carried out as explained in Section "Applications of the TH-λ Plot: Ideal examples". For instance, the gel, coke, and intermediate λ-line are shown in Figure 9. The NTH-line for exchanger E05AB after the clean gradually moves from the reference gel λ-line to the coke λ-line, indicating significant deposit ageing after months 3-4. The asymptotic loss of duty performance is however seriously outpaced by the rapid increase in pressure drop.

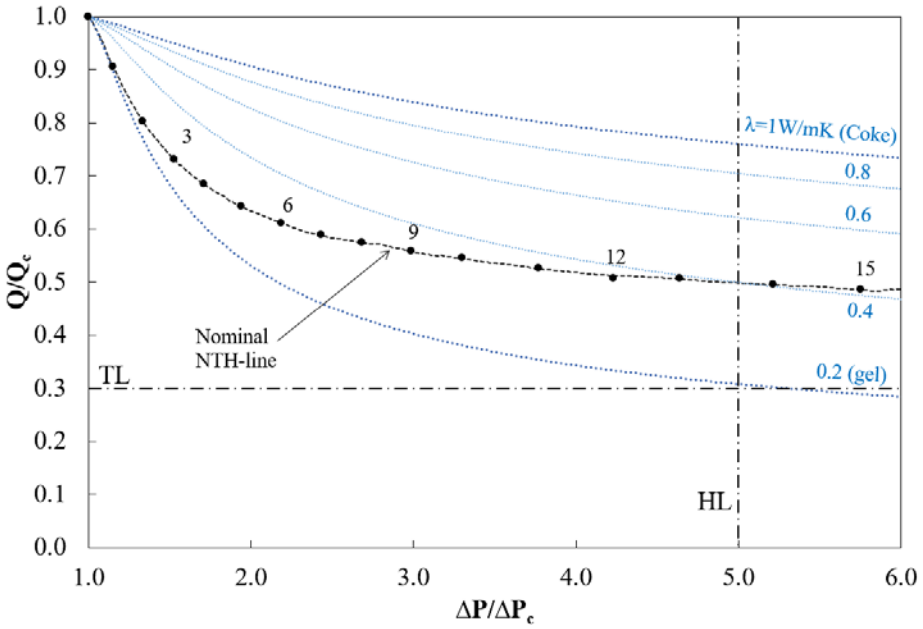

Figure 9: TH-λ Plot with Nominal NTH-line for E05AB-P3.

TH-λ PLOT WITH INDUSTRIAL REFINERY DATA

In this section, the TH-λ concept is demonstrated with actual measured plant data. The practical application of the full TH-λ concept requires the availability of measured inlet conditions of flowrate and temperature, heat duty, Q and tube-side pressure drop, ΔP. Q is calculated from measured flowrate and inlet and outlet temperatures; ΔP is directly measured. The TH-line resulting from Q and ΔP from

refinery measurements involve both process variability *and* measurement error and is affected by the evolution and properties of the fouling layer. As indicated earlier, if the measurement noise is significant, an intermediate smoothing step may be required to facilitate the reading and interpretation of the graph.

The example in this section considers heat exchanger E155AB, described in Section "Heat Exchangers used in the Examples". Temperatures, flowrates *and tube-side pressure drops* were measured for a period of 42 months of operation. Therefore, simultaneous monitoring of thermal and hydraulic performance is possible. A single operation period was available. As no previous plant data is available, the Nominal conditions were extracted from the same operating period.

Before discussing the TH-λ Plot, and for illustration purposes, the TH-line before the normalization step is shown with and without the intermediate smoothing step in Figure 10. In all cases, due to the long duration of the period, data are emphasized and labelled every three months (rather than monthly). The *raw* TH-line (Figure 10a) provides the general trend in the performance of the unit without further manipulation of the data. However, the noise in the pressure drop measurements introduces fluctuations in the X axis, making it difficult to follow the time evolution of the performance as fouling builds up (indeed, the "line" is more like a cloud of points!). The ΔP measurement noise was significant, with a standard deviation of 0.22 bar (5-10%). The smoothing of the apparent deposit characteristics was performed with a moving average (as explained and shown in ref.[55]). The smoothed TH-line (Figure 10b) presents reduced fluctuations in the X axis, greatly facilitating the reading and interpretation of the graph. The error bars are displayed for the tri-monthly points used as temporal labels.

The TH-line, once normalized, can be displayed on top of the map composed by a number of λ-lines, as shown in Figure 11(a), where λ-lines are shown for various increments of λ within the typical range for organic deposits (0.2 – 1 $Wm^{-1}K^{-1}$) and above, to λ =1.6 $Wm^{-1}K^{-1}$. At the beginning of the operation, following a cleaning of the exchanger, the performance is close to clean conditions (position [1,1] in the plot). The HL and TL limits are defined at 3.0 and 0.3, respectively. However, they are not shown in Figure 11(a) as they are still far from the current operating conditions. The monitoring of this heat exchanger over time and information obtained are discussed in the following.

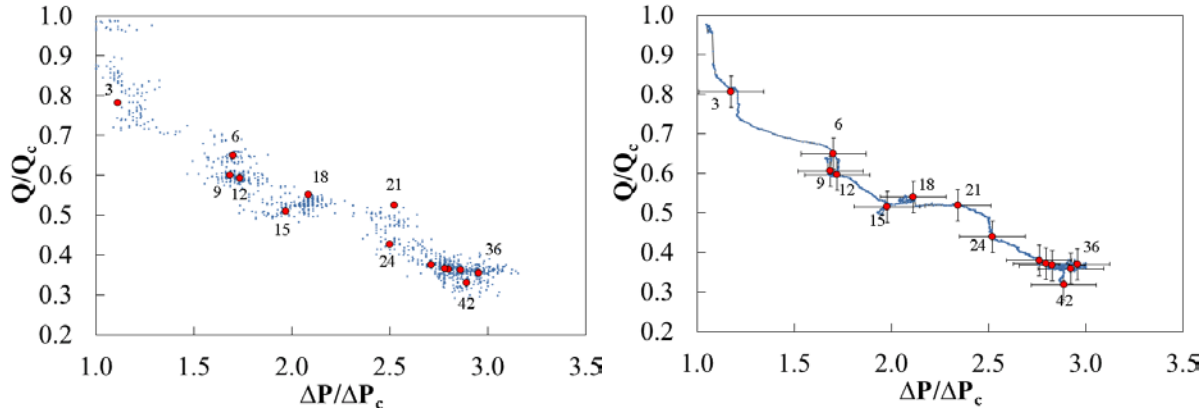

(a) (b)

Figure 10. TH-line for E155AB: (a) with raw duty and pressure drop; (b) with smoothing of apparent thickness and conductivity. Dots indicate data every 3 months.

During the initial three months (Figure 11a), the operator observes a reduction on both the thermal and hydraulic performance. The thermal performance presents smaller uncertainty at this stage. It is clear that heat recovery has decreased to around 80% of the clean duty. This indicates that fouling is building up fast, which is not completely unexpected when operation re-starts following a mechanical cleaning. The pressure drop has also decreased, although the uncertainty in the X axis does not allow extracting definitive conclusions on the percentage increase, nor on the conductivity of the deposit. The position of the measured performance hints that the deposit conductivity could be above 0.5 W/mK. At this early stage, organic fouling is unlikely to have aged at the operating conditions of this unit. Hence, this could be an indication of mixed organic-inorganic fouling.

During the fourth month of operation (between points “3” and “4” in Figure 11b), the exchanger seems to continue fouling at a similar rate, with a further reduction in thermal performance of 5% of the clean duty. The hydraulic performance does not seem to be significantly affected. However, during the fifth month of operation (between points “4” and “5” in Figure 11b) there is a very fast increase in pressure drop of ca. 20% of the clean one. The thermal performance is not as severely affected as the hydraulic one. As a result, the NTH-line clearly moves to higher conductivities that are approaching fast the “coke line”. This indicates fast deposition of inorganic matter is most likely happening. Given the location of the exchanger, in between the desalter and the pre-flash, this could well be due to

inorganics breakthrough from the desalter. With this information in hand, the operator could check operations immediately and take action before the situation worsened.

During the sixth month of operation (between points “5” and “6” in Figure 11c, where a change of scale on the x-axis is noted) this trend continues, with the performance going down to 65% of the clean duty and 170% of the clean pressure drop. Therefore, the pressure drop has increased by 50% of the clean value in less than two months. Around 6 months the deposit conductivity reaches a maximum value of 1.2-1.4 $Wm^{-1}K^{-1}$. These values are well above the coke line and confirm the acute deposition of inorganic matter over the previous two months of operations. Indeed, had corrective measurements been taken between months 4 – 5, based on the information already available then, such acute fouling build-up in the unit could possibly have been avoided.

After that, the unit performance stabilizes for another 6 months (between points “6” and “12” in Figure 11d). During this period the thermal performance decreases by ca. 5%, but the hydraulic performance does not seem affected. This indicates either that there is little deposition of a low conductive material or, more likely, that some of the highly conductive inorganic material deposited earlier is now being removed and replenished by deposit of lower conductivity. During the three months that follow (between points “12” and “15” in Figure 11e), fouling starts building up again at a moderate rate, with the conductivity showing a small decreasing trend. This indicates that deposition is building up as it used to before the fast deposition period between months 4-6. Between months 15 and 19 (points “15” and “19” in Figure 11e), fouling stabilizes again and does not seem to progress. Duty and pressure drops are about 50% and twice, respectively, of their clean value.

Between months 19 and 21 (points “19” and “21” in Figure 11f), there seems to be a second inorganic-dominated fouling period, as indicated by the relative position of the TH-line with respect to the λ-lines. The increase of pressure drop is of 30% of the clean value during these two months. At this stage, small amounts of deposit have a greater impact on pressure drop than at the beginning of the operation, when the exchanger is cleaner. As a result, this indicates a likely second episode of inorganic breakthrough, but not as severe as the one observed between months 4 and 6. Between months 21 and 24, there is a clear change in trend toward lower deposit conductivities, which points to a period of organic-dominated deposition.

After that, and until the end of month 27 (2 years and 3 months of operation, Figure 11g), fouling shows again a moderate build-up with gradually decaying conductivity, similarly to the behaviour observed between months 12 and 15. After 27 months the thermal performance is 38% of the clean duty and the hydraulic performance is 270% of the clean pressure drop. Both stabilize around those values until the end of the operating period (42 months, Figure 11h). The apparent conductivity stays at values of 0.6 – 0.8 $Wm^{-1}K^{-1}$ until the end of the operating period. This indicates that either the organic fraction of the deposit does not age significantly or that there is some replenishment of material, whereby higher conductive fouling is removed, and low conductive fouling continues depositing. Operation of the unit is by now quite close to both its thermal and hydraulic limits (and indeed it was then cleaned).

Overall, focusing on the evolution of fouling, the monitoring of the unit using the method presented would have revealed an acute deposition period between months 4 and 6, possibly due to inorganics breakthrough. From that point onwards, the overall trend is towards lower conductivities as the deposit grows, which could be interpreted as a change in fouling behaviour toward less conductive deposits, most likely due to a more dominant presence of organic deposition as the tube clogs. This trend is only interrupted in the period between 15 – 21 months, which shows again a medium-fast increase in pressure drop and stable duty, reaching a local maximum in conductivity of about 1 – 1.2 $Wm^{-1}K^{-1}$. The two maxima in deposit conductivity seem to be preceded by a similar trend in the TH-line with fast deposition and towards high conductivities and points to periods of inorganic-dominated fouling.

It should be noted that the inlet operating conditions are much more stable than in the previous example (E05AB), and consequently the TH-line did not show significant fluctuations in the Y axis (Figure 10b). In fact, the fluctuations due to measurement error were greater than those due to process variability, and the operating band (not shown here) is within the error bar shown for trimonthly data. Therefore, here the smoothed TH-line (Figure 10b) is very similar to the NTH-line (Figure 11), and in this example the smoothing step is more important than the normalization step.

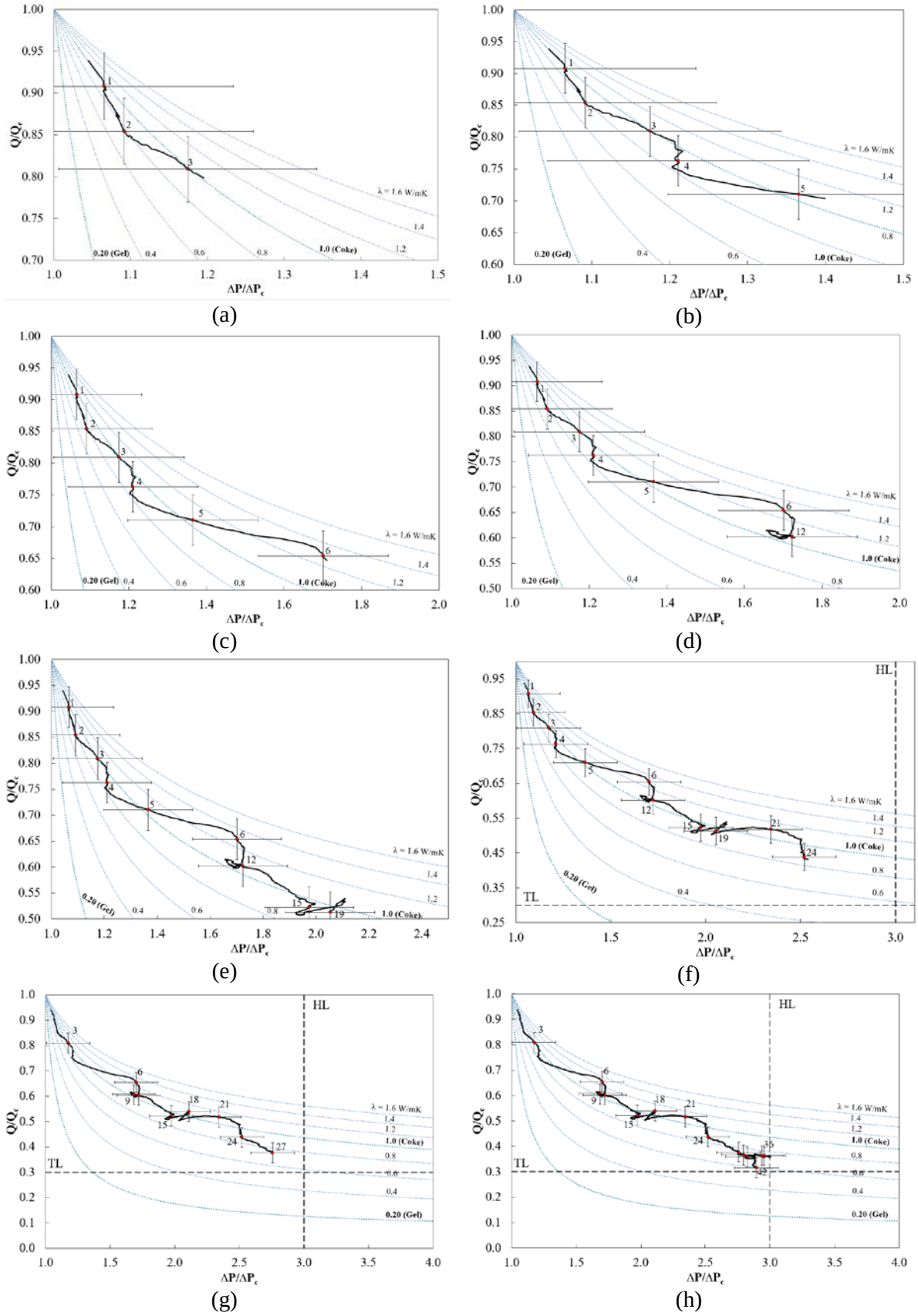

Figure 11: TH-λ Plot for E155AB at month 3(a), month 5 (b), month 6 (c), month 12 (d), month 19 (e), month 24 (f), month 27 (g) and month 42 (h).

DISCUSSION AND CONCLUSIONS

A new model-based monitoring approach of heat exchangers undergoing fouling, the dynamic thermo-hydraulic TH-λ method, has been presented. Simultaneous consideration of thermal and hydraulic performance, together with process dynamics, was shown to be essential to adequately monitor and interpret available data. This was demonstrated through a number of ideal cases and a real industrial refining case study with historical plant data. The novel graphical representation provides unique capabilities to visualise the current and predicted performance of a single exchanger relative to that expected in clean and various reference conditions. The evolution of the fouling behaviour so evidenced provides the operator/engineer with a rapid diagnostic of the phenomena occurring within the unit and motivates a more detailed analysis, if so required.

The proposed normalization method removes the effect of process variability (inlet temperatures and flowrates) on the assessed performance of the unit in the TH space. Although this normalization was aimed at enabling the generation of the TH-λ Plot, it can also be useful to define the range of expected thermal and hydraulic performance within specified confidence levels. This is the area delimited by the NTH-lines for maximum and minimum temperature driving force (according to the characteristic variability in the inlet conditions). Such dynamic analysis may be used in practice to provide insights and limiting performance bounds which are very useful for performance monitoring, event diagnosis, process control and operations optimisation.

Once the process variability has been removed, the TH-λ Plot and reference conductivity λ-lines are very useful to: a) simultaneously evaluate and trend the interacting thermal and hydraulic performance over time, under reference or predicted inlet conditions; b) highlight underlying mechanisms contributing to overall performance, such as fouling rate and ageing; c) detect deviations from predicted performance due to changes from expected fouling behaviour; d) help in the identification of potential fouling causes. This analysis provides a very rich set of information and enables an early response from engineers, which may be to take adequate remedial actions, or if necessary, conduct a more detailed analysis. It should be noted that the comparison of the thermal-

hydraulic performance with λ-lines is strictly valid if the shell-side fouling is negligible. Otherwise, the conductivity indicated by the relative position of the NTH-line would be under-estimated.

The model-based monitoring method presented relies heavily on the use of detailed dynamic, distributed models of the type described. They enable the systematic exploitation of primary data(measurements of temperatures, flowrates and pressure drops) and generation of the plots by performing a number of complex tasks: a) estimation of the clean performance of the heat exchanger under time-varying conditions; b) decoupling the variations in heat exchanger performance due to process variability from those due to changes in fouling rates and/or deposit properties; c) smoothing of the TH-line in order to facilitate the reading and interpretation of the graphs; d) predicting the thermo-hydraulic behaviour of the heat exchanger as fouling builds up; e) if pressure drops are not measured, using the models as pressure drop soft-sensors.

The monitoring approach presented achieves a comprehensive analysis of primary plant measurements that allows extracting a huge amount of additional information on both fouling and operational aspects. This information is conveyed effectively by the visualization plot of past and predicted performance, utilising easy to understand indicators of underlying fouling, and highlighting useable trends and performance bounds. The industrial examples presented demonstrate that the model-based data analysis method and visualisation plot enable detecting and diagnosing unexpected operational events. They should be valuable in planning, optimising and controlling corrective operational decisions with respect to fouling mitigation options and cleaning strategies.

ACKNOWLEDGMENTS

Initial methodological aspects of this research were partially performed under the UNIHEAT project, for which EDB and SM wish to acknowledge the Skolkovo Foundation and BP for financial support. Hexxcell Ltd. for the provision of Hexxcell Studio™ is also acknowledged.

NOMENCLATURE

A = Analysis type (acronym)

A = Flow area, m^2

A_a = Ageing constant, s^{-1}

b = Cleaning binary variable, -

c = Mass concentration, kg m^{-3}

CF = Cleanliness factor, -

C_f = Friction factor, -

CIT = Coil inlet temperature, ºC

COT = Coil outlet temperature, ºC

C_p = Specific heat capacity, J kg^{-1} K^{-1}

dir = Direction of flow, -

E_f = Fouling deposition activation energy, J mol^{-1}

FI = Fouling index, -

FIT = Furnace inlet temperature, ºC (equivalent to CIT)

h = Heat transfer coefficient, J m^2K^{-1}

H = Specific enthalpy, J kg^{-1}

HEX = Heat exchanger

HL = Hydraulic limit

L = Tube length, m

$LMTD$ = Log-mean temperature difference, ºC

$\dot{m}$ = Mass flowrate, kg s^{-1}

$MaxDF$ = Maximum driving force line

$MinDF$ = Minimum driving force line

$NFIT$ = Normalized furnace inlet temperature, ºC

n = Fouling rate, kg m^{-2} s^{-1}

NC = Number of components

NCl = Number of cleanings

N_p = Number of tube passes

NR = Number of reactions

NTH = Normalized thermo-hydraulic

P = Prediction type

PHT = Pre-heat train

PTH = Predicted thermo-hydraulic

p = Perimeter, m

P = Pressure, Pa

$P1, \mathrm{P3}$ = Period 1, Period 3

p_i = Inorganic-to-organic deposition rate ratio of component *i*

Pr = Prandtl number

Q = Heat duty, W

$q"$ = Heat flux, W m^{-2}

R = Tube radius, m

R_{flow} = Flow radius, m

Re = Reynolds number

R_f = Fouling resistance, m^2 K W^{-1}

R_g = Ideal gas constant, J mol^{-1} K^{-1}

r = Radial coordinate, m

$\tilde{r}$ = Dimensionless radial coordinate, -

r_j = Rate of reaction j, kg m^{-3} s^{-1}

T, t = Hot fluid, cold fluid temperature, K

t = Time, s

T_{film} = Tube-side film temperature, K

TH = Thermo-hydraulic

TL = Thermal limit

U = Overall heat transfer coefficient, W m^{-2} K^{-1}

u = Linear velocity, m s^{-1}

x = Volume fraction, m^3 m^{-3}

z = Axial coordinate, m

Greek letters

α' = Deposition constant, kg m^{-2} s^{-1}

γ' = Removal constant, kg m^{-2} s^{-1} Pa^{-1}

ΔP = Pressure drop, Pa

ΔT = Temperature difference, ºC

δ = Fouling layer thickness, m

ε = Thermal effectiveness, -

$\dot{\delta}_l$ = Rate of change of fouling layer thickness, m s^{-1}

λ = Thermal conductivity, W m^{-1} K^{-1}

ρ = Density, kg m^{-3}

σ = Standard deviation, K

ν = Stoichiometric coefficient, -

τ = Wall shear stress, N m^{-2}

Ω = Spatial domain

Subscripts

a = Apparent
ave = Average
c = Clean
eff = Effective
f = Fouling
gel = Fresh organic deposit
i = Component number, inner radius
in = Inlet
j = Reaction number
l = Fouling layer
max = Maximum
n = Pass number

o = Outer
out = Outlet
ref = Reference
s = Shell-side flow
t = Tube-side flow
tot = Total
w = Tube wall

REFERENCES

(1) Macchietto S.; Hewitt G.F.; Coletti F.; Crittenden B.D.; Dugwell D.R.; Galindo A.; Jackson G.; Kandiyoti R.; Kazarian S.G.; Luckham P.F.; Matar O.K.; Millan-Agorio M.; Muller E.A.; Paterson W.; Pugh S.J.; Richardson S.M.; Wilson D.I. Fouling in Crude Oil Preheat Trains: A Systematic Solution to an Old Problem. *Heat Transf Eng*. **2011**;32(3-4):197-215. doi:10.1080/01457632.2010.495579.

(2) Coletti F.; Joshi H.M.; Macchietto S.; Hewitt G.F. Introduction to Crude Oil Fouling. In: Coletti F.; Hewitt G.F., eds. *Crude Oil Fouling: Deposit Characterization, Measurements, and Modeling*. Boston: Gulf Professional Publishing (Elsevier); 2014.

(3) Jerónimo M. A. S., Melo L. F., Sousa Braga A., Ferreira P. J. B. F., and Martins C., Monitoring the thermal efficiency of fouled heat exchangers: A simplified method, *Exp. Therm. Fluid Sci.*, vol. 14, no. 4, pp. 455–463, 1997.

(4) EPRI, *EPRI NP-7552 Heat Exchanger Monitoring guidelines*, 1991.

(5) ASME, *ASME OM-S/G-1994 Standard and Guides for Operation and Maintenance of Nuclear Power Plants*, 1995.

(6) Kuppan T., *Heat exchanger design handbook*. New York: Marcel Dekker, 2000.

(7) Waters A. J., Akinradewo C. G., and Lamb D., Fouling: Implementation of a Crude Preheat Train Performance Monitoring Application at the Irving Oil Refinery, in *International Conference on Heat Exchanger Fouling and Cleaning VIII*, 11-19 June, Schladming, Austria; **2009**: pp. 33–38.

(8) Heins A., Veiga R., Ruiz C., and Riera A., Fouling Monitoring and Cleaning Optimisation in a Heat Exchanger Network of a Crude Distallation Unit, *Proc. 7th Int. Conf. Heat Exch. Fouling*

Clean. - Challenges Oppor., vol. RP5, no. 1925, 2007.

(9) Mozdianfard M. R. and Behranvand E., A field study of fouling in CDU preheaters at Esfahan refinery, *Appl. Therm. Eng.*, vol. 50, no. 1, pp. 908–917, Jan. 2013.

(10) Chunangad K., Chang R., Curcio L., and Casebolt R., Consider thermal and hydraulic impacts of fouling in crude preheat exchanger design, in *AIChE Spring Meeting and 12th Global Congress on Process Safety*, Houston, USA; April 10-14, 2016, p. 186b.

(11) Watkinson A. P., *Particulate Fouling of Sensible Heat Exchangers*, University of British Columbia, 1968.

(12) Wilson D. I. and Watkinson A. P., A study of autoxidation reaction fouling in heat exchangers, *Can. J. Chem. Eng.*, vol. 74, pp. 236–246, 1996.

(13) Turakhia M., Characklis W. G., and Zelver N., Fouling of Heat Exchanger Surface: Measurement and Diagnosis, *Heat Transf. Eng.*, vol. 5, no. July 2015, pp. 93–101, 1984.

(14) Albert F., Augustin W., and Scholl S., Roughness and constriction effects on heat transfer in crystallization fouling, *Chem. Eng. Sci.*, vol. 66, no. 3, pp. 499–509, 2011.

(15) Radhakrishnan, V.R., Ramasamy, M., Zabiri, H., Do Thanh, V., Tahir, N.M., Mukhtar, H., Hamdi, M.R., Ramli, N., Heat exchanger fouling model and preventive maintenance scheduling tool, *Appl. Therm. Eng.*, vol. 27, no. 17–18, pp. 2791–2802, Dec. 2007.

(16) Rafeen M. S., Mohamed M. F., Mamot M. Z., Manan N. A., Shafawi A., and Ramasamy M., Crude Oil Fouling : Petronas Refineries Experience, in *Engineering*, 2010, pp. 4–8.

(17) Wilson D. I., Polley G. T., and Pugh S. J., Mitigation of Crude Oil Preheat Train Fouling by Preheat Train Fouling, *Heat Transf. Eng.*, vol. 23, no. August 2013, pp. 24–37, 2002.

(18) Zubair S. M., Sheikh A. K., Younas M., and Budair M. O., A risk based heat exchanger analysis subject to fouling Part I : Performance evaluation, vol. 25, pp. 427–443, 2000.

(19) Yeap B. L., Wilson D. I., Polley G. T., and Pugh S. J., Mitigation of crude oil refinery heat exchanger fouling through retrofits based on thermo-hydraulic fouling models, *Chem Eng Res Des*, vol. 82, no. A1, pp. 53–71, 2004.

(20) Liporace F. S. and De Oliveira S. G., Real Time Fouling Diagnosis and Heat Exchanger Performance, *Heat Transf. Eng.*, vol. 28, no. 3, pp. 193–201, Mar. 2007.

(21) Şahin G., Orman S., Becer M., Ayhan U. B., Özçelik Y., and Balkan F., Fouling Monitoring in Diesel Unit Preheat Exchangers, in *Proceedings of International Conference on Heat Exchanger Fouling and Cleaning 2011*. Crete Island, Greece; 2011, pp. 57–61.

(22) Markowski M., Trafczynski M., and Urbaniec K., Identification of the influence of fouling on the heat recovery in a network of shell and tube heat exchangers, *Appl. Energy*, vol. 102, pp. 755–764, Feb. 2013.

(23) Ishiyama E. M., Pugh S. J., Paterson W. R., Polley G. T., Kennedy J., and Wilson D. I., Management of Crude Preheat Trains Subject to Fouling, *Heat Transf. Eng.*, vol. 34, no. 8–9, pp. 692–701, Jul. 2013.

(24) Astorga-Zaragoza C.-M., Zavala-Río A., Alvarado V. M., Méndez R.-M., and Reyes-Reyes J., Performance monitoring of heat exchangers via adaptive observers, *Measurement*, vol. 40, no. 4, pp. 392–405, 2007.

(25) Mohanty D. K. and Singru P. M., Use of C-factor for monitoring of fouling in a shell and tube heat exchanger, *Energy*, vol. 36, no. 5, pp. 2899–2904, May 2011.

(26) Ratel M., Kapoor Y., Anxionnaz-Minvielle Z., Seminel L., and Vinet B., Investigation of fouling rates in a heat exchanger using an innovative fouling rig, in *Proc. Int. Conf. Heat Exchanger Fouling and Cleaning - 2013*, Budapest, Hungary, 2013, pp. 36–41.

(27) Coletti F. and Macchietto S., Refinery Pre-Heat Train Network Simulation Undergoing Fouling: Assessment of Energy Efficiency and Carbon Emissions, *Heat Transf. Eng.*, vol. 32, no. 3–4, pp. 228–236, Mar. 2011.

(28) GE, *Refinery Process Fouling Control*, 2012.

(29) Bories M. and Patureaux T., Preheat Train Crude Distillation Fouling Propensity Evaluation by the Ebert and Panchal Model, in *Proc. ECI Conf. on Heat Exchanger Fouling and Cleaning: Fundamentals and Applications*, 2003, pp. 200–210.

(30) Negrão C. O. R., Tonin P. C., and Madi M., Supervision of the thermal performance of heat exchanger trains, *Appl. Therm. Eng.*, vol. 27, no. 2–3, pp. 347–357, Feb. 2007.

(31) Baker Hughes, *LIFESPAN Exchanger Fouling Control Program*, 2011.

(32) Ishiyama E. M., Paterson W. R., and Wilson D. I., Platform for Techno-economic Analysis of

Fouling Mitigation Options in Refinery Preheat Trains, *Energy & Fuels*, vol. 23, no. 3, pp. 1323–1337, Mar. 2009.

(33) Lohr K. R. and Rose J. L., Ultrasonic guided wave and acoustic impact methods for pipe fouling detection, *J. Food Eng.*, vol. 56, no. 4, pp. 315–324, 2003.

(34) Merheb B., Nassar G., Nongaillard B., Delaplace G., and Leuliet J. C., Design and performance of a low-frequency non-intrusive acoustic technique for monitoring fouling in plate heat exchangers, *J. Food Eng.*, vol. 82, no. 4, pp. 518–527, 2007.

(35) Müller-Steinhagen H., Malayeri M. R., and Watkinson A. P., Heat Exchanger Fouling: Mitigation and Cleaning Strategies, *Heat Transf. Eng.*, vol. 32, no. 3–4, pp. 189–196, Mar. 2011.

(36) Hewitt G. F., Shires G. L., and Bott T. R., *Process heat transfer*. London: CRC press, 1994.

(37) Gunness R. C. and Baker J. G., Testing heat transfer equipment, *Ind. Eng. Chem.*, vol. 30, no. 4, pp. 373–376, 1938.

(38) Jones G. M. and Bott T. R., Monitors and models for the assessment of petroleum fouling of refinery heat exchangers, in *Proc. Int. Conf. Mitigation of Heat Exchanger Fouling and its Economic and Environmental Implications, July 18-23, 1999, Banff, Canada*, 2001, pp. 59–69.

(39) Glen N. F., Howarth J. H., and Jenkins A. M., Fouling monitoring on process plant - field experience, in *Int. Conf. Mitigation of Heat Exchanger Fouling and its Economic and Environmental Implications, July 18-23, 1999, Banff, Canada*, 2001, pp. 70–76.

(40) Takemoto T., Crittenden B. D., and Kolaczkowski S. T., Interpretation of fouling data in industrial shell and tube heat exchangers, *Chem. Eng. Res. Des.*, vol. 77, no. 8, pp. 769–778, 1999.

(41) Coletti F.; Crittenden B.D.; Haslam A.J.; Hewitt G.F.; Jackson G.; Jimenez-Gutierrez G.; Macchietto S.; Matar O.K.; Müller E.A.; Sileri D.; and Yang J. Modelling of Fouling from Molecular to Plant Scale. In: Coletti F, Hewitt GF, eds. *Crude Oil Fouling: Deposit Characterization, Measurements, and Modeling*. Boston: Gulf Professional Publishing; 2014.

(42) Crittenden B. D., Kolaczkowski S. T., and Downey I. L., Fouling of Crude Oil Preheat Exchangers, *Trans IChemE, Part A, Chem Eng Res Des*, vol. 70, pp. 547–557, 1992.

(43) Mirsadraee A. and Malayeri M. R., Analysis of Highly Noisy Crude Oil Fouling Data Using Kalman Filter, in *Proc. Int. Conf. Heat Exchanger Fouling and Cleaning - 2015*, 2015, pp. 97–103.

(44) Diaz-Bejarano E., Coletti F., and Macchietto S., Impact of Complex Layering Structures of Organic and Inorganic Foulants on the Thermohydraulic Performance of a Single Heat Exchanger Tube: A Simulation Study, *Ind. Eng. Chem. Res.*, vol. 55, no. 40, 2016.

(45) Diaz-Bejarano E., Coletti F., and Macchietto S., Crude Oil Fouling Deposition, Suppression, Removal, and Consolidation—and How to Tell the Difference, *Heat Transf. Eng.*, vol. 38, no. 7–8, 2017.

(46) ESSCo, *Normalisation in Monitor, a trademark of Nalco Company*, 2008. .

(47) Ishiyama E. M., Paterson W. R., and Wilson D. I., The Effect of Fouling on Heat Transfer, Pressure Drop, and Throughput in Refinery Preheat Trains: Optimization of Cleaning Schedules, *Heat Transf. Eng.*, vol. 30, no. 10–11, pp. 805–814, Sep. 2009.

(48) Ishiyama E. M., Paterson W. R., and Wilson D. I., Thermo-hydraulic channelling in parallel heat exchangers subject to fouling, *Chem. Eng. Sci.*, vol. 63, no. 13, pp. 3400–3410, Jul. 2008.

(49) Díaz-Bejarano E.; Coletti F.; Macchietto S. Detection of Changes in Fouling Behavior by Simultaneous Monitoring of Thermal and Hydraulic Performance of Refinery Heat Exchangers. *Computer Aided Chemical Engineering*. **2015**, 37:1649-1654. doi:10.1016/B978-0-444-63577-8.50120-0.

(50) Díaz-Bejarano E.; Coletti F.; Macchietto S. Model-Based Monitoring of Thermal-Hydraulic Performance of Refinery Heat Exchangers Undergoing Fouling. *Computer Aided Chemical Engineering*. **2016**, 38:1911-1916. doi:10.1016/B978-0-444-63428-3.50323-4.

(51) Hexxcell Ltd. Hexxcell Studio. http://www.hexxcell.com, 2019.

(52) Coletti F.; Macchietto S. A Dynamic, Distributed Model of Shell-and-Tube Heat Exchangers Undergoing Crude Oil Fouling. *Ind Eng Chem Res*. **2011**;50(8):4515-4533.

(53) Diaz-Bejarano E.; Coletti F.; Macchietto S. A new dynamic model of crude oil fouling deposits and its application to the simulation of fouling-cleaning cycles. *AIChE J*. **2016**;62(1). doi:10.1002/aic.15036.

(54) Diaz-Bejarano E.; Coletti F.; Macchietto S., Thermo-hydraulic analysis of refinery heat exchangers undergoing fouling, *AIChE J.*, vol. 63, no. 3, 2017.

(55) Diaz-Bejarano E., Behranvand E., Coletti F., Mozdianfard M. R., and Macchietto S., Organic and inorganic fouling in heat exchangers – Industrial case study: Analysis of fouling state, *Appl. Energy*, vol. 206, pp. 1250–1266, 2017.

(56) Panchal C.B.; Kuru W.C.; Liao C.F.; Ebert W.A.; Palen J.W. Threshold conditions for crude oil fouling. In: Bott T.R.; Melo L.F.; Panchal C.B.; Somerscales E.F.C., eds. *Understanding Heat Exchanger Fouling and Its Mitigation*. New York: Begell House; **1999**:273-279.

(57) Zabiri H., Radhakrishnan V. R., Ramasamy M., Ramli N., Thanh V. D., and Wah C. S., Development of heat exchanger fouling model and preventive maintenance diagnostic tool, *Chem. Prod. Process Model.*, vol. 2, no. 2, 2007.

(58) Müller-Steinhagen H., *Handbook of Heat Exchanger Fouling: Mitigation and Cleaning Technologies*. Essen, Germany: Publico Publications, 2000.

(59) Wang W.; Watkinson A.P. Iron Sulphide and coke fouling from sour oils: review and initial experiments. In: Malayeri MR, Müller-Steinhagen H, Watkinson AP, eds. *Int. Conf. on Heat Exchanger Fouling and Cleaning 2011*. Vol **2011**. Crete Island, Greece; 2011:23-30.

(60) Diaz-Bejarano E., Coletti F., and Macchietto S., “Beyond Fouling Factors: a Reaction Engineering Approach to Crude Oil Fouling Modelling,” in *Int. conf. on heat exchanger fouling and cleaning 2015*, Enfield (Dublin), Ireland, June 7 - 12, 2015, pp. 89 - 96.

(61) Coletti F., Diaz-Bejarano E., Martinez J., and Macchietto S., “Heat exchanger design with high shear stress: reducing fouling or throughput?,” in *Int. conf. on heat exchanger fouling and cleaning 2015*, Enfield (Dublin), Ireland, June 7 - 12, 2015, pp. 27-33.

(62) Holman J. P., *Heat transfer*, 8th ed. London: McGraw-Hill, 2001.

(63) Saunders E. A. D., *Heat exchangers: Selection, Design, and Construction*. Longman, Harlow, 1988.

(64) Taborek J., Shell-and-tube heat exchangers: single phase flow, in *Heat Exchanger Design Handbook*, G. F. Hewitt, Ed. New York: Begell House, 2002.

(65) Diaz-Bejarano E., Coletti F. and Macchietto S., A Novel Way of Monitoring Heat Exchanger

Performance: the Dynamic TH-λ Plot, presentation 480245 at 2017 AIChE Spring Conference, San Antonio, TX, USA, 28 March 2017.

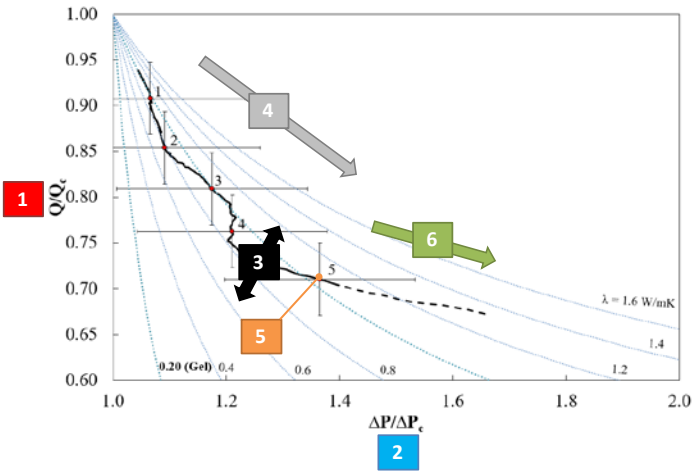

TH-λ PLOT
HEAT EXCHANGER AND FOULING MONITORING

1 THERMAL PERFORMANCE (T)

2 HYDRAULIC PERFORMANCE (H)

3 FOULING LAYER PROPERTIES (λ)

4 PAST EVOLUTION

5 DIAGNOSIS OF CURRENT STATE, EVENTS AND TRENDS

6 PERFORMANCE PREDICTION